Studienrichtung Vermessung und Geoinformation
Technische Universität Wien

GEOWISSENSCHAFTLICHE MITTEILUNGEN

Heft 64

A Primer of Geodesy
for GIS Users

Second, revised and extended edition

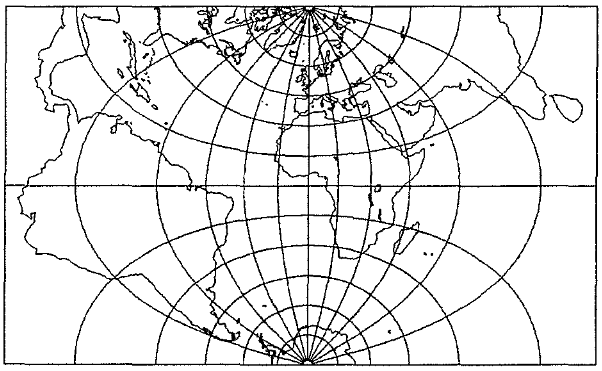

Universal Transverse Mercator Projection

Kurt Bretterbauer & Robert Weber
Institute of Geodesy and Geophysics, Dept. of Advanced Geodesy

Geowiss. Mitt. 64, 2003

Vienna, Fall 2003

Impressum:

Responsible for the contents:

Prof. em. Dr. Kurt Bretterbauer
Prof. Dr. Robert Weber

e-mails: kbretter@luna.tuwien.ac.at
rweber@luna.tuwien.ac.at

Printed by: Hochschülerschaft TU Wien
Wirtschaftsbetriebe GmbH
A-1040 Wien

Edition: 100 copies

Expenses for printing and binding: Deptartment of Advanced Geodesy

A Primer of Geodesy

A Primer of Geodesy

0 Preface

In recent years Geodesy has become an essential part of the background of GIS. It originated in attempts to justify rigorously certain operational rules. The following essay is designed for use as a supplement to textbooks on GIS. To use geodetic ideas and techniques, the user must know what he is doing and why, not merely how. The authors thought the best approach to be a mixture of algebraic, graphical, and numerical presentation of the topics discussed. A set of solved problems serves to illustrate the theory. It is recommended to work them out independently on a PC or by hand computation with a pocket calculator. We hope the text is appropriate for a general audience.

All geodetic data are affected by errors, ideally by random errors only. Generally, the data are the result of an adjustment process based on the theory of probability. The following treatise does not deal with data quality but endeavours to give some mathematical background for the correct handling of geodetic data in geoinformation systems. The free accessibility to automatically recording instruments and to relevant software animated people of different background to work in GIS, many of them without even a basic knowledge of geodesy. The worst consequence often is the total absence of any statement on data quality, and about what is called 'geodetic datum', i.e. the coordinate and height system in use. Problems also occur, when data have to be linked which are based on different geodetic datums or different map projections. It is essential always to check the quality of data, and which system they are referred to. The following essay is meant to help avoiding loss of information and accuracy between the acquisition of data and their processing in GISs.

Geodesy strictly works within the SI-system of physical units [m-kg-s]. Though modern techniques of position fixing with the Global Positioning System (GPS) have to account for relativistic effects, the geometrical and physical structure of our world of cognition is represented sufficiently accurate by Euclidian geometry and Newtonian mechanics. The reader is asked always to remember that truth can only be approximated, sometimes more, sometimes less, and that bad data can't be improved in GIS.

1 Geodesy in General

Geodesy is a natural as well as a technical science. It is that branch of applied mathematics and physics which determines, by observations and measurements, the size and shape of the Earth, its gravity field, and the coordinates of points in special coordinate systems. Concerning geoinformatics we might say: Geodesy collects and administrates all data necessary for the description of the geometrical and physical structure of the Earth's surface and of near-earth space, and provides these data in analogous or digital form to potential users. The definition and realization of coordinate systems and their interrelations are basic problems of geodesy [1], [2], [3], [4].
Geodesy deals with no less than nine different surfaces (*Figure 1.1*): The solid Earth surface (lithosphere), the sea surface (hydrosphere), the surface of the ice caps (cryosphere), the manifold of equipotential surfaces (level surfaces), the geoid, the

telluroid, the quasi-geoid, several individual reference ellipsoids, and the Mean Earth Ellipsoid (MEE).

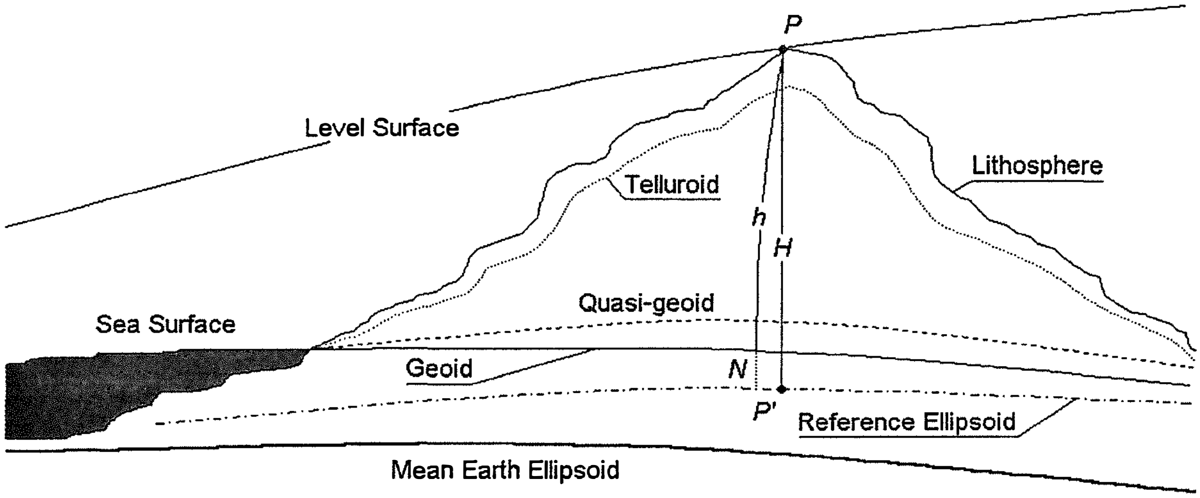

Figure 1.1

At least five of these surfaces are of relevance for GISs, i.e. the physical Earth surface, the MEE and individual ellipsoids as reference surfaces for position, the geoid and the quasi-geoid as reference surfaces for heights. Monitoring of the sea surface and the surface of the ice caps becomes increasingly important in view of a possible climate change, a real challenge for satellite altimetry.

1.1 Methodical Setup of Geodesy

The methodical setup of geodesy is demonstrated in a simple diagram.

GEODESY

↓

Mathematical Geodesy (including map projections)	Physical Geodesy (gravity field research)	Cosmic Geodesy (including satellite positioning)

↓ ↓ ↓ ↓

National Surveys (including geoinformation systems)	Plane Surveying (including civil engineering)

Each of these partial disciplines defines and uses special coordinate systems and runs its own data banks. **Note!** Contrary to surveying and because of the connection with time angles in geodesy are reckoned in degrees (24 h = 360°, 1° = 4 min).

Depending on various demands the results of geodetic operations are represented in different models. There is a fundamental distinction between geodesy and surveying.

Whereas geodesy aims to determine the gravity field, surveying tries to abstract from its effects. In terms of information theory we can say: A signal for geodesy, is noise for surveying. We have to distinguish between three stages of approximation for the figure of the Earth: The sphere, the ellipsoid, and the geoid. A sphere of radius R = 6371.0 km might suffice for many purposes. If it is used as a basis of a data bank this fact has to be made clear explicitly. As it is, the Earth's departure from a sphere is too great for geodesy. The next best approximation is the oblate ellipsoid of revolution, occasionally but not quite correctly also named 'spheroid'. The ellipsoid is simple enough so that computations are not overly difficult.

Of great significance in geodesy are the level surfaces, i.e. surfaces of equal gravitational potential. Geometrically they are defined as surfaces being everywhere normal to the direction of the plumb line. The consequence is that between two points on one and the same level surface water cannot flow, or put in other words, the surface of any liquid in rest is part of a level surface. There is a particular one out of the infinite manifold of level surfaces surrounding the Earth which nearly coincides with mean sea level, and that is named the 'Geoid' (the term was coined in the 19th century by the German mathematician *Listing*).

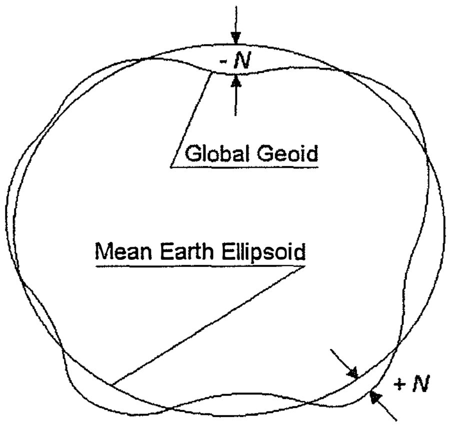

Figure 1.2: Sketch of the MEE and the geoid, exaggerated

On the continents the geoid runs inside the Earth's crust and it serves as a reference surface for a special height system. Because of visible and invisible mass irregularities the geoid is a very complicated surface which cannot be represented by an analytical equation but only by its discrete distances (the geoid undulations N) from a well defined ellipsoid (*Figure 1.2*). Like the physical Earth surface the geoid is unsuitable as a mathematical model for computations. Yet, the detailed determination of the geoid is one of the most pressing and painstaking problems of geodesy. In the near future the global geoid may be known to 1 - 2 cm with wave length of about 100 km.

As the geoid is warped, geodesy had to find an ellipsoid which most nearly approximates the geoid with the least departure therefrom. The MEE (also called 'level ellipsoid') is the closest reasonable approximation to the figure of the Earth, geometrically as well as physically. It is a mathematically created artificial body, rigorously defined by only four parameters whose numerical valus are taken from the real Earth body: The semi-major axis a, the product of gravitational constant times mass of the Earth GE, the socalled dynamic flattening J_2, and the angular velocity of the Earth rotation ω. All other parameters can rigorously be derived from these four quantities, like the geometric flattening f, the excentricity e^2, the semi-minor axis b, the potential U_0 and the gravity values at the equator and the poles.

By historical and practical reasons every country uses its own regional 'reference ellipsoid'. These reference ellipsoids differ considerably from the MEE in dimension and in position with respect to the Earth body. While the MEE is a representative for the whole Earth, the reference ellipsoids were only meant to approximate a particular region. Consequently, the distances of the geoid from a reference ellipsoid are called relative undulations, and those from the MEE absolute ones. The relative undulations usually amount to only a few meters, but the absolute undulations reach up to ± 100 m.

Nowadays the detailed knowledge of the geoid becomes increasingly important for large technical constructions like long tunnels under mountain ranges or for particle accelerators.

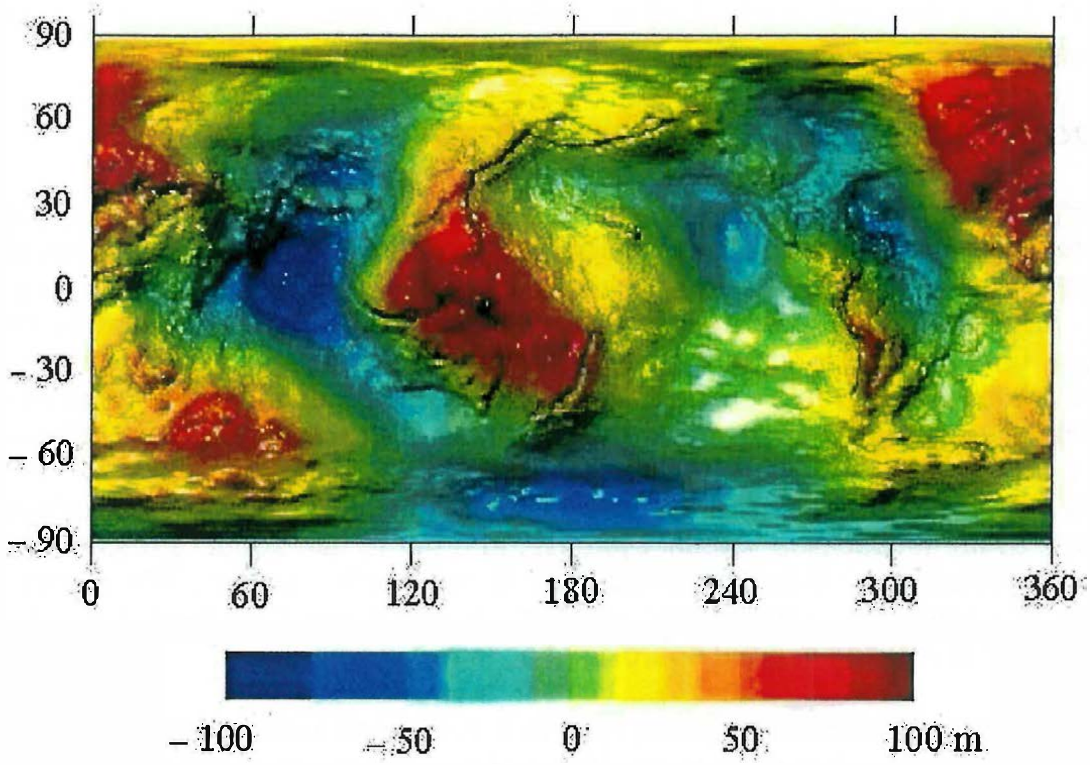

Figure 1.3: Global Geoid – EGM96

1.2 Geodetic Models for GIS

We have to distinguish between several models as bases of geoinformation systems:

Global geodetic 3D-model
(3D-cartesian coordinates)

↓

3D-hybrid model =
= global or regional 2D-geometric model (ellipsoidal coordinates)
plus physically defined height model

↓

2D-models obtained by conformal mapping onto the plane

Classical geodesy frequently was called 'two-dimensional' because determinations of position and of height have been separate operations on principle. GPS now made the simultaneous determination of all three cartesian spatial coordinates possible. Yet, still

2D-surface (i.e. ellipsoidal) coordinates have to be interposed as 3D-cartesian coordinates can neither be directly converted into plane coordinates nor is it possible to derive technically useful heights from them. It is quite easy to derive heights above the MEE from GPS data. But what you want, especially in navigation, are heights above sea level. Those can only be obtained by a combination with the geoidal undulationes *N* (cf. Chapter 6).

2 Coordinates and their Transformation

Our world of cognition can be objectified as a sequence of events in time and space. The term ‘time’ may be taken as an appropriate name for the world-wide connection of all events. Time is one-dimensional, space is three-dimensional, in order to pinpoint a location we need a triple of numbers called coordinates. All material points are subject to motion, hence, coordinates are time-dependent on principle. The distinction of time and position is fundamental: A material body may occupy the same position at different times but never different positions at the same time, which fact sometimes is ignored.

The laws of Newtonian mechanics are simple, however, only in non-accelerated coordinate systems, socalled ‘inertial systems’. In order to talk about terrestrial systems we have to know how they are embedded in an inertial system. We recognize a hierarchy of coordinate systems with geodesy as regulating discipline. The supreme inertial system is realized in good approximation in two ways:

- By a conventional kinematic system fixed to a number of extra-galactic radio sources (quasars), and to fundamental stars. This system presently is represented by a list of positions of more than 200 quasars at standard epoch 2000.0, and by the positions and proper motions of 118 218 stars of the Hipparcos Catalogue at epoch 1991.25. The precise positions of those extragalactic objects materialize the socalled International Celestial Reference Frame (ICRF). The Hipparcos Catalogue provides only an optical reference linked to the ICRF.
- By a conventional dynamic system based on the dynamical properties of the motion of bodies of the solar system, i.e. planets, the Moon, and artificial satellites. This system is realized by the orbital ephemerides of the relevant object.

Earth-fixed coordinate systems are not inertial because they are rotating. Rotating systems are characterized by the phenomenon of virtual forces (Coriolis and centrifugal force).

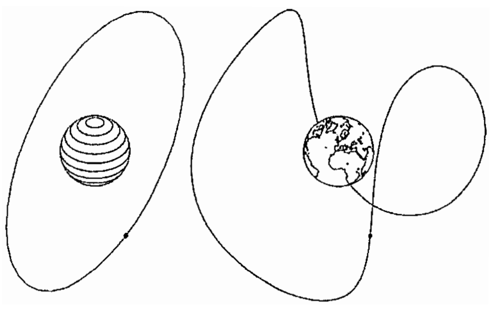

Figure 2.1a *Figure 2.1b*

In everyday life it is hard to discern between motion in an Earth-fixed and in an inertial frame. However, the significant distinction between inertial and terrestrial systems can be demonstrated by the orbital motion of one of the NAVSTAR satellites. *Figure 2.1a* shows the orbit of a GPS-satellite as seen in the inertial system with the Earth rotating in the orbital plane. *Figure 2.1b* shows the identical orbit now seen from an Earth-fixed point of view.

Any method which uses a set of numbers to fix a point or an object in space is called a coordinate system. We have to distinguish between the ideal concept of such a system and its realization in the physical world. The first notion actually means the ‘coordinate system', the second the 'coordinate frame'. The latter is represented by a set of fixpoints. The relative positions of fixpoints, however, is unknown unless the metric of the space extended by the coordinate system is given. This becomes obvious with the 'natural coordinates', which are the parameters of the gravity field: astronomical latitude and longitude, and potential difference. Without detailed knowledge of the metric of the gravity field one cannot calculate the distance or the direction between two points. Even if the metric were known, calculations would be extremely difficult and not very accurate.

In order to meet all demands of potential users several coordinate systems are defined with preference of orthogonal systems. Not every coordinate system suits every demand. The definition of a coordinate system for a special purpose results from a convention of its users. Hence, we talk about 'conventional coordinate systems'. The simplest and widest used coordinate system is the orthogonal cartesian system. A point in its space is given by the position vector:

(2.1) $$\mathbf{x} = \begin{pmatrix} x_1 \\ x_2 \\ x_3 \end{pmatrix} = x_1\mathbf{e}_1 + x_2\mathbf{e}_2 + x_3\mathbf{e}_3 = \sum_{i=1}^{3} x_i\mathbf{e}_i, \quad \text{where} \quad \mathbf{e}_i \cdot \mathbf{e}_j = \delta_{ij} = \begin{cases} 0 & \text{if } i \neq j \\ 1 & \text{if } i = j \end{cases}.$$

As can be seen, the metric is that of Euclidian space. It might be useful to mention that in problems connected with deformation analysis orthogonal systems are not best suited. Here, generalized systems should be used. The appropriate mathematical tool is tensor calculus [5] which is outside the scope of this treatise.

2.1 Transformation of Cartesian Coordinate Systems

Many problems in geodesy are nothing else than transformations of coordinate systems. Transformations of cartesian systems are generally composed of a translation of the origin, of one or more rotations, and of at least one scale factor. Such transformations are subject to certain conditions, like: conservation of straight lines, of parallelism, and of proportions. The most general transformation is a linear mapping called affine transformation. It satisfies the above conditions, but the scale depends on the orientation of a line, i.e. parallel lines have the same scale. Angles and thus the form of a figure, however, are changed. Mathematically the affine transformation is given by 12 parameters, for whose unique (minimal) determination four common points in both systems must be known. For each point we have the equations:

(2.2) $$\begin{pmatrix} x' \\ y' \\ z' \end{pmatrix} = \underbrace{\begin{pmatrix} \delta x \\ \delta y \\ \delta z \end{pmatrix}}_{\text{translation vector}} + \underbrace{\begin{pmatrix} a_{11} & a_{12} & a_{13} \\ a_{21} & a_{22} & a_{23} \\ a_{31} & a_{32} & a_{33} \end{pmatrix}}_{\text{rotation matrix}} \cdot \begin{pmatrix} x \\ y \\ z \end{pmatrix}.$$

The rotation matrix implicitly contains three scale factors. Therefore, affine transformations are not much used in geodesy where conformal transformations are preferred. Yet, (2.2) is very useful for determining approximate values of the parameters of the similitude transformation, and of course, (2.2) should be used in deformation analysis.

The constraint on the transformation can be tightend by demanding a conformal mapping, which conserves angles. Recently, *Grafarend* [6] gave a simple robust, conformal 10-parameter transformation near identity which leaves angles and distance ratios locally unchanged. It is useful in special cases where only small rotation angles occur. Note that this method should only be applied in small areas and that it does not contain a change in scale. Let $\mathbf{x} = [x_1, x_2, x_3]^T$, $\mathbf{y} = [y_1, y_2, y_3]^T$ be the coordinates of the two systems to be transformed and $\mathbf{t} = [t_1, t_2, t_3, t_4, t_5, t_6, t_7, t_8, t_9, t_{10}]^T$ the vector of the transformation-parameters. Then the following equation holds:

(2.2a)

$$\begin{bmatrix} 1 & 0 & 0 & -x_2 & -x_3 & 0 & -x_1^2 + x_2^2 + x_3^2 & -2x_1x_2 & -2x_1x_3 & x_1 \\ 0 & 1 & 0 & x_1 & 0 & -x_3 & -2x_1x_2 & x_1^2 - x_2^2 + x_3^2 & -2x_2x_3 & x_2 \\ 0 & 0 & 1 & 0 & x_1 & x_2 & -2x_1x_3 & -2x_2x_3 & x_1^2 + x_2^2 - x_3^2 & x_3 \end{bmatrix} \cdot \begin{bmatrix} t_1 \\ t_2 \\ t_3 \\ t_4 \\ t_5 \\ t_6 \\ t_7 \\ t_8 \\ t_9 \\ t_{10} \end{bmatrix} = \mathbf{y} - \mathbf{x}.$$

The transformation generally used in geodesy is the '7-parameter similitude transformation'. Here, as with the affine transformation, rotation angles of any size are permitted. There is only one scale factor, the transformation is conformal. First, we discuss only the rotations abstracting from the shift of the origin (*Figure 2.2*).

For checking computations it is useful to remember that the rotation matrix is orthogonal, i.e.:

(2.3) $\mathbf{R}^{-1} = \mathbf{R}^T, \quad \det|r_{ij}| = 1.$

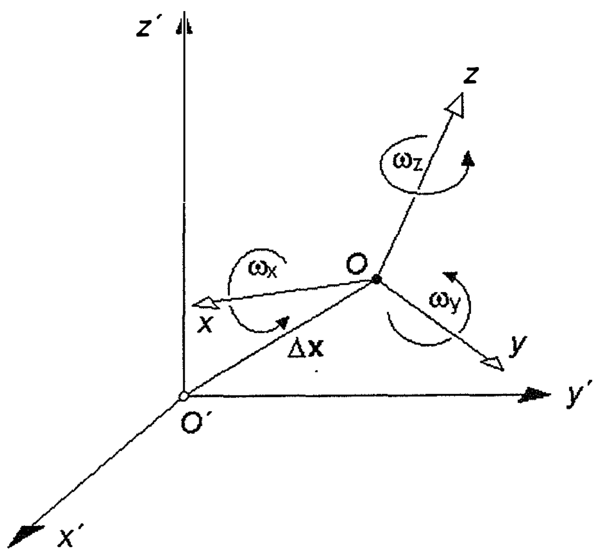

Figure 2.2

A rotation is marked positive when executed counter-clockwise looking along the axis towards the origin. A single rotation about the *x*-, or the *y*-, or the *z*-axis is mathematically expressed by one of the following matrices (abbreviating, '*c*' stands for cosine and '*s*' for sine).

(2.4)
$$\mathbf{R}_x = \begin{pmatrix} 1 & 0 & 0 \\ 0 & c\omega_x & s\omega_x \\ 0 & -s\omega_x & c\omega_x \end{pmatrix}, \quad \mathbf{R}_y = \begin{pmatrix} c\omega_y & 0 & -s\omega_y \\ 0 & 1 & 0 \\ s\omega_y & 0 & c\omega_y \end{pmatrix}, \quad \mathbf{R}_z = \begin{pmatrix} c\omega_z & s\omega_z & 0 \\ -s\omega_z & c\omega_z & 0 \\ 0 & 0 & 1 \end{pmatrix}.$$

If two orthogonal matrices are multiplied the product is an orthogonal matrix too, i.e. the combination of two or three rotations again is a rotation. Note that in a succession of rotations the next rotation always is about the new axes. Generally, three rotations are performed. Principally, there are six possible successions of rotations, namely:

$$\mathbf{R}_z\mathbf{R}_y\mathbf{R}_x, \quad \mathbf{R}_z\mathbf{R}_x\mathbf{R}_y, \quad \mathbf{R}_y\mathbf{R}_z\mathbf{R}_x, \quad \mathbf{R}_y\mathbf{R}_x\mathbf{R}_z, \quad \mathbf{R}_x\mathbf{R}_z\mathbf{R}_y, \quad \mathbf{R}_x\mathbf{R}_y\mathbf{R}_z.$$

When the first rotation is about the x-axis, the next about the new y-axis, and the third about the new z-axis then the total rotation matrix reads:

(2.5)
$$\mathbf{R} = \mathbf{R}_z\mathbf{R}_y\mathbf{R}_x = \begin{pmatrix} c\omega_y c\omega_z & s\omega_x s\omega_y c\omega_z + c\omega_x s\omega_z & -c\omega_x s\omega_y c\omega_z + s\omega_x s\omega_z \\ -c\omega_y s\omega_z & -s\omega_x s\omega_y s\omega_z + c\omega_x c\omega_z & c\omega_x s\omega_y s\omega_z + s\omega_x c\omega_z \\ s\omega_y & -s\omega_x c\omega_y & c\omega_x c\omega_y \end{pmatrix}.$$

Note! Different successions of rotations lead to different results as can be demonstrated by a simple example. A dice may be rotated by 90° about the y-axis (in the first plot perpendicular to the paper), and then again by 90° about the new z-axis (*Figure 2.3a*). In a second trial we swap the successions of rotations, the result being quite different (*Figure 2.3b*).

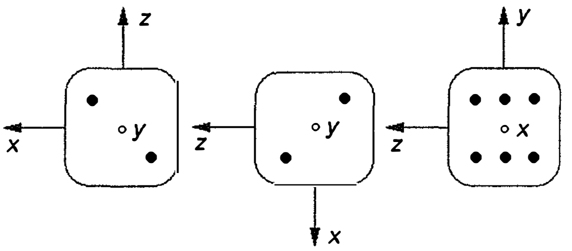

Figur 2.3a

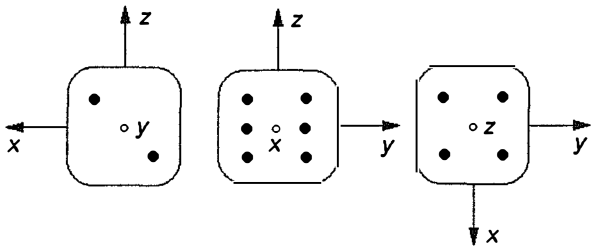

Figur 2.3b

By the way, three successive rotations about three axes can be substituted by one single rotation about one single axis which fact is of significance in robotics. This axis is found by asking for the manifold of points which by the original three rotations are mapped upon themselves.

In star-astronomy (not in satellite geodesy) only rotations occur, but in geodesy we also have to deal with a translation of the origin and with a scale factor m. Hence a complete 7-parameter transformation reads:

(2.6) $$\begin{pmatrix} x' \\ y' \\ z' \end{pmatrix} = \begin{pmatrix} \delta x \\ \delta y \\ \delta z \end{pmatrix} + (1+m)\cdot \mathbf{R} \cdot \begin{pmatrix} x \\ y \\ z \end{pmatrix}, \quad \text{or for short} \quad \mathbf{x}' = \delta\mathbf{x} + (1+m)\cdot \mathbf{R} \cdot \mathbf{x}.$$

The scale factor m is to be introduced in ppm, i.e. mm per km. Equation (2.6) represents what in geodesy is called the 'spatial *Helmert*-transformation'. In the geodetic literature it is also termed the '*Bursa-Wolf* model'. When converting a local network into the geocentric system the rotations are strongly correlated with the components of the shift vector, because over the long distance to the geocenter a rotation nearly is identical with a translation. The socalled '*Molodensky-Badekas* model' avoids this trouble by reducing the coordinates to their barycenters, which corresponds to a shift.

When converting a regional geodetic system into a global geocentric one the rotational angles generally are quite small (a few seconds of arc). In that case the total rotation matrix (2.5) reduces to the simple form (the angles, of course, have to be introduced in radians):

(2.7) $$\mathbf{R} = \begin{pmatrix} 1 & \omega_z & -\omega_y \\ -\omega_z & 1 & \omega_x \\ \omega_y & -\omega_x & 1 \end{pmatrix}.$$

However, one should make sure that the demanded accuracy is maintained by this simplification.

Sometimes a change in orientation of one or the other axis becomes necessary. This is achieved by 'mirror matrices':

(2.8) $$\mathbf{S}_x = \begin{pmatrix} -1 & 0 & 0 \\ 0 & 1 & 0 \\ 0 & 0 & 1 \end{pmatrix}, \quad \mathbf{S}_y = \begin{pmatrix} 1 & 0 & 0 \\ 0 & -1 & 0 \\ 0 & 0 & 1 \end{pmatrix}, \quad \mathbf{S}_z = \begin{pmatrix} 1 & 0 & 0 \\ 0 & 1 & 0 \\ 0 & 0 & -1 \end{pmatrix}.$$

2.2 Determination of Transformation Parameters

The determination of the seven transformation parameters requires at least three identical points in both coordinate systems. The one set of coordinates may come from a classical triangulation net, the other one from GPS-observations. This gives nine linear equation for the seven unknowns, and we are confronted with a problem of least squares adjustment. We only consider the simplified case with small rotation angles (otherwise we had to introduce approximate values for the rotation angles). The set of equations reads:

(2.9a) $$\begin{pmatrix} x' \\ y' \\ z' \end{pmatrix} = \begin{pmatrix} \delta x \\ \delta y \\ \delta z \end{pmatrix} + (1+m)\cdot \begin{pmatrix} 1 & \omega_z & -\omega_y \\ -\omega_z & 1 & \omega_x \\ \omega_y & -\omega_x & 1 \end{pmatrix} \cdot \begin{pmatrix} x \\ y \\ z \end{pmatrix}.$$

First we have to linearize the product (1 + m)**R** neglecting terms small of second order:

$$(1+m)\cdot\begin{pmatrix} 1 & \omega_z & -\omega_y \\ -\omega_z & 1 & \omega_x \\ \omega_y & -\omega_x & 1 \end{pmatrix} = \begin{pmatrix} 1+m & \omega_z & -\omega_y \\ -\omega_z & 1+m & \omega_x \\ \omega_y & -\omega_x & 1+m \end{pmatrix} = \begin{pmatrix} 1 & 0 & 0 \\ 0 & 1 & 0 \\ 0 & 0 & 1 \end{pmatrix} + \begin{pmatrix} m & \omega_z & -\omega_y \\ -\omega_z & m & \omega_x \\ \omega_y & -\omega_x & m \end{pmatrix}.$$

Now we apply the *Molodensky-Badekas* model by reducing the coordinates of both systems to their barycenters which fact is characterized by the subscript 's'. Then equations (2.9a), fully developed, read:

$$\begin{aligned} x'_s &= mx_s - \omega_y z_s + \omega_z y_s + x_s, \\ y'_s &= my_s + \omega_x z_s - \omega_z x_s + y_s, \\ z'_s &= mz_s - \omega_x y_s + \omega_y x_s + z_s. \end{aligned} \tag{2.9b}$$

The vector of corrections then is:

$$\mathbf{v} = \begin{bmatrix} 1 & 0 & 0 & x_s & 0 & -z_s & y_s \\ 0 & 1 & 0 & y_s & z_s & 0 & -x_s \\ 0 & 0 & 1 & z_s & -y_s & x_s & 0 \\ \bullet & \bullet & \bullet & \bullet & \bullet & \bullet & \bullet \end{bmatrix} \cdot (0,0,0,m,\omega_x,\omega_y,\omega_z)^{\mathrm{T}} - \begin{bmatrix} x'_s - x_s \\ y'_s - y_s \\ z'_s - z_s \\ \bullet \end{bmatrix} = \mathbf{Au} - \ell. \tag{2.10}$$

The dots indicate that the matrix and the vector have to be extended accordingly depending on the number of identical points. For three identical points **A** is a 9 × 7-matrix and ℓ a 9-element vector, in case of four identical points we have a 12 × 7-matrix and a 12-element vector, a.s.o. The rotation angles and the scale factor then follow from the relation:

$$\mathbf{u} = \left(\mathbf{A}^{\mathrm{T}}\mathbf{A}\right)^{-1}\mathbf{A}^{\mathrm{T}}\,\ell = (0,0,0,m,\omega_x,\omega_y,\omega_z)^{\mathrm{T}}. \tag{2.11}$$

The shift vector finally results from the difference: barycenter of the target system minus barycenter of the original one (i.e. primed system minus unprimed).

2.3 Homogeneous Coordinates

By introducing socalled 'homogeneous coordinates' the three operations: rotation, translation, and scaling can be put into a consistent form quite convenient for programming. A point in 3D-space can be represented by a quadrupel of numbers which are determined only up to a common factor: $x, y, z \to r, s, t, u$. The interrelation between cartesian and homogeneous coordinates are then given by:

$$x = s/r, \quad y = t/r, \quad z = u/r. \tag{2.12}$$

The new coordinates are termed 'homogeneous' because all algebraic relations in cartesian coordinates when converted to homogeneous coordinates become homogeneous. The simplest form is obtained if we put r = 1. Then a point in 3D-space is represented by the vector $\mathbf{x} = \mathbf{x}(1, x, y, z)$. The idea of this measure is to put the 7-parameter transformation in a very concise form where only products of 4 × 4-matrices occur. The matrices for rotation $\mathbf{R}_x, \mathbf{R}_y, \mathbf{R}_z$ and those for shift **T** and scale **M** then become:

$$\mathbf{R}_x = \begin{pmatrix} 1 & 0 & 0 & 0 \\ 0 & 1 & 0 & 0 \\ 0 & 0 & c\omega_x & s\omega_x \\ 0 & 0 & -s\omega_x & c\omega_x \end{pmatrix}, \quad \mathbf{R}_y = \begin{pmatrix} 1 & 0 & 0 & 0 \\ 0 & c\omega_y & 0 & -s\omega_y \\ 0 & 0 & 1 & 0 \\ 0 & s\omega_y & 0 & c\omega_y \end{pmatrix}, \quad \mathbf{R}_z = \begin{pmatrix} 1 & 0 & 0 & 0 \\ 0 & c\omega_z & s\omega_z & 0 \\ 0 & -s\omega_z & c\omega_z & 0 \\ 0 & 0 & 0 & 1 \end{pmatrix},$$

(2.13) $$\mathbf{T} = \begin{pmatrix} 1 & 0 & 0 & 0 \\ \delta x & 1 & 0 & 0 \\ \delta y & 0 & 1 & 0 \\ \delta z & 0 & 0 & 1 \end{pmatrix}, \quad \mathbf{M} = \begin{pmatrix} 1 & 0 & 0 & 0 \\ 0 & 1+m & 0 & 0 \\ 0 & 0 & 1+m & 0 \\ 0 & 0 & 0 & 1+m \end{pmatrix}.$$

The total transformation now reads:

(2.13a) $$\mathbf{x}' = \mathbf{T} \cdot \mathbf{M} \cdot \mathbf{R}_z \cdot \mathbf{R}_y \cdot \mathbf{R}_x \cdot \mathbf{x}.$$

3 The Hierarchy of Coordinate Systems

Modern geodesy works in an Earth-fixed geocentric cartesian coordinate system. The geocenter can be determined only indirectly but quite accurately by dynamic methods of satellite geodesy. As the rotational axis of the Earth body is subject to complicated motions we have to distinguish between several coordinate systems:

- **The Conventional Inertial System** (CIS). The origin is in the geocenter, its Z^0-axis coincides with the axis of angular momentum at the standard epoch J2000.0 (2000, January 1, 12h UT), the X^0-axis points to the vernal equinox as represented by the positions of the fundamental quasars. These celestial fixpoints form the Conventional Inertial Reference Frame (IRF).

- **The Conventional Terrestrial System** (CTS). The origin is in the geocenter, its *Z*-axis points to the mean pole of the years 1900 – 1905 (called Conventional International Origin CIO), the *X,Z*-plane lies in the mean meridian of Greenwich.The realization of that system is called International Terrestrial Reference Frame (ITRF) and is defined by a number of fundamental stations equipped with Satellite Laser Ranging, GPS-receivers, and some with radio telescopes. The phenomenon of plate tectonics causes variations of the coordinates of these stations so that the ITRF has to be redefined periodicly. A two-digit annex tells about the year of the update, e.g. ITRF 96.

Transformation between these two systems is performed by several rotation matrices considering precession and nutation of the rotational axis, phase of Earth rotation (sidereal time), and polar motion. Data necessary for this transformation are provided by the International Earth Rotation Service (IERS). More details are beyond the scope of this treatise (cf. [7]).

- **World Geodetic System 84** (WGS84). This is the system GPS is working in since 1987. It combines the cartesian system CTS with the MEE of the Geodetic Reference System 1980 (GRS80) and a representation of the Earth's gravitational potential in form of a harmonic expansion up to order and degree 180 (with 32 755 coefficients).
- **Parametry Zemli 1990** (PZ90). PZ90 (Earth Parameter System 1990) is the designation of the coordinate system of the Russian satellite navigation system GLONASS. Similar to the WGS84 the PZ90 acts since 1993 as reference system for GLONASS broadcast orbit information. PZ90 is of a quality comparable to the WGS84 but it is realized by a very small number of reference station, all of them located in the territory of the Russian Federation. Upcoming realizations of the PZ90 will be based on a real global network of monitoring sites.
- **Regional Surveying Systems**. Many countries still work with regional coordinate systems and reference ellipsoids which are rotated and translated with respect to the ITRF (*Figure 3.1*). A regional geodetic datum uses an ellipsoid which best approximates the geoid in that particular region. This ellipsoid is fixed in some manner to the Earth body at some fundamental point in the region. The conversion to the ITRF or vice versa is done by the 7-parameter transformation. When such a regional geodetic datum was established it was tried to bring the minor axis of the ellipsoid as close as possible to the rotational axis of the Earth, and the x,y-plane parallel to the Greenwich meridian. Hence, the rotation angles are generally rather small. The shift vector $\Delta\mathbf{x}$ however usually amounts to several hundred meters.

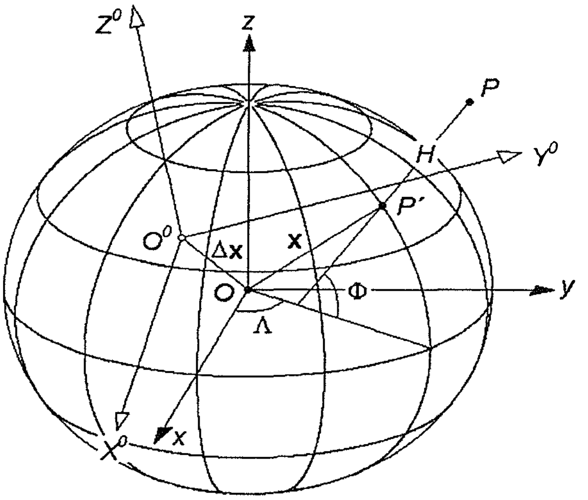

Figure 3.1: Reference ellipsoid and ITRF strongly exaggerated

Since about 1850 many different ellipsoids have been defined, e.g. the ellipsoids of *Everest, Bessel, Clarke, Hayford, Krassovskij*, to name only a few. Many of them are still in use, like the ellipsoid of *Bessel* in Austria, Germany, Switzerland and some other countries, like in parts of Asia.

Just to give an idea about typical transformation parameters those for the transformation of ITRF into the Austrian Datum MGI (Military Geographical Institute) may be stated:

Scale factor: $m = -2.5$ ppm.

$$\textit{shift vector:}\quad \begin{matrix} \delta x = -575\,\text{m} \\ \delta y = -93\ \text{m}\,, \\ \delta z = -466\,\text{m} \end{matrix} \qquad \textit{rotation angles:}\quad \begin{matrix} \omega_x = 5.1'' \\ \omega_y = 1.6''\,, \\ \omega_z = 5.2'' \end{matrix}$$

Warning! In most cases such parameters are averaged values representative for a large area, giving an accuracy of only a few meters. That's why the above shift vector is given only to full meters. Never let you be deceived by the number of digits behind the decimal point. It is no definit sign of precision. When working on the centimeter level individual parameters for smaller areas have to be determined which might differ considerably from the averaged ones. The neglect of this fact often becomes the source of a loss of information and accuracy.

3.1 Ellipsoidal Coordinates

An oblate ellipsoid of revolution is generated by rotating an ellipse about its minor axis. Hence, it is sufficient to examine a meridian curve of the ellipsoid to understand its geometry (*Figure 3.2*). The ellipse, and the ellipsoid also, is defined by two parameters i.e. the major axis *a* and the minor axis *b*. The equation of an ellipsoid in a cartesian system with origin in the center and *z*-axis in the minor axis is given by:

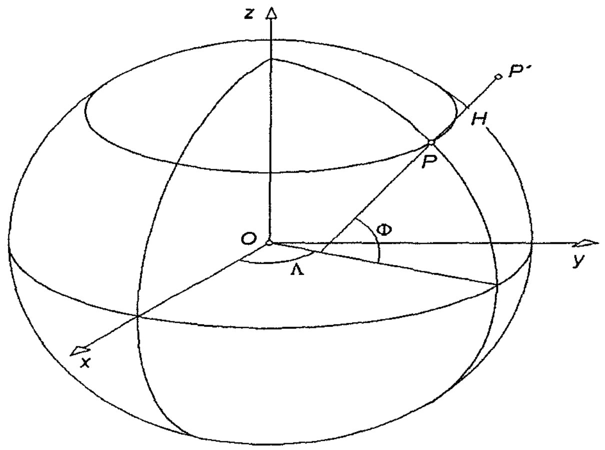

Figure 3.2: Geometry of the Ellipsoid

$$\frac{x^2+y^2}{a^2}+\frac{z^2}{b^2}=1. \tag{3.1}$$

For practical computations several auxiliary parameters have been defined as functions of *a* and *b*: *f* = flattening, *e* = first excentricity, *e′* = second eccentricity, *c* = radius of polar curvature.

$$\begin{aligned} &f=\frac{a-b}{a}, \quad b=a(1-f), \quad c=\frac{a^2}{b}, \\ &e^2=\frac{a^2-b^2}{a^2}, \quad e'^2=\frac{a^2-b^2}{b^2}. \end{aligned} \tag{3.2}$$

A point in space is given in terms of the ellipsoidal coordinates: 'geodetic latitude' Φ, 'geodetic longitude' Λ, and 'ellipsoidal height' *H*. Φ is the angle between the normal to the ellipsoid and the *x*,*y*-plane (equatorial plane), Λ the angle between the relevant meridian plane and the *x*,*z*-plane (usually in the Greenwich mean meridian), and *H* is the normal distance from the ellipsoid. The geodetic or ellipsoidal latitude and longitude resp. must not be mixed up with the astronomical latitude and longitude which give the direction of the natural plumb line. The difference between both types of parameters is the 'deflection of the vertical'. It depends on the irregularities of the gravity field and on the ellipsoid chosen, and can amount up to 30 seconds of arc or more.

With the aid of another auxiliary quantity $V=\sqrt{1+e'^2\cos^2\Phi}$ the transformation of ellipsoidal coordinates to the cartesian system (3.1) is given by the formulae:

$$x = \left(\frac{c}{V} + H\right)\cos\Phi\cos\Lambda,$$

(3.3) $$y = \left(\frac{c}{V} + H\right)\cos\Phi\sin\Lambda,$$

$$z = \left[\left(1 - e^2\right)\frac{c}{V} + H\right]\sin\Phi.$$

The inverse transformation is not quite so easy. Λ follows directly from

(3.4) $$\Lambda = \arctan(y/x).$$

Solving equations (3.3) for Φ and H is theoretically possible but very complicated. In practice it is done by iteration starting with $H = 0$, or by an approximate solution which nevertheless is very accurate (cf. [7], p. 258). With the auxiliary terms Θ and p defined by:

(3.5) $$\Theta = \arctan\left(\frac{az}{bp}\right), \quad p = \sqrt{x^2 + y^2},$$

latitude and height result from

(3.6) $$\Phi = \arctan\left(\frac{z + e'^2 b \sin^3\Theta}{p - e^2 a \cos^3\Theta}\right), \quad H = \frac{p}{\cos\Phi} - \frac{c}{V}.$$

Note that two normals of the ellipsoid subtending the tiny angle of 1" intersect the ellipsoid in two points 30 m apart. In order to keep millimeter accuracy, latitude and longitude thus have to be given to 0.0001" or to $(3 \cdot 10^{-8})°$.

For many computations in a limited area the ellipsoid can be substituted by an 'osculating sphere' which is assumed tangent to the ellipsoid in a central point of the region. The radius of this sphere is equal to the geometric mean of the principal radii of the ellipsoid:

(3.7) $$R = c/V^2.$$

V has to be calculated for the latitude of the tangent point.

3.2 Local Geodetic System

Such systems may become relevant when terrestrially observed data must be handled in GISs. The origin of such a system is some fixpoint on the Earth's surface P (*Figure 3.3*). The w-axis is assumed to be the normal of the reference ellipsoid, the u-axis pointing to geodetic north, and the v-axis to the east. This system is also termed 'horizon system'.

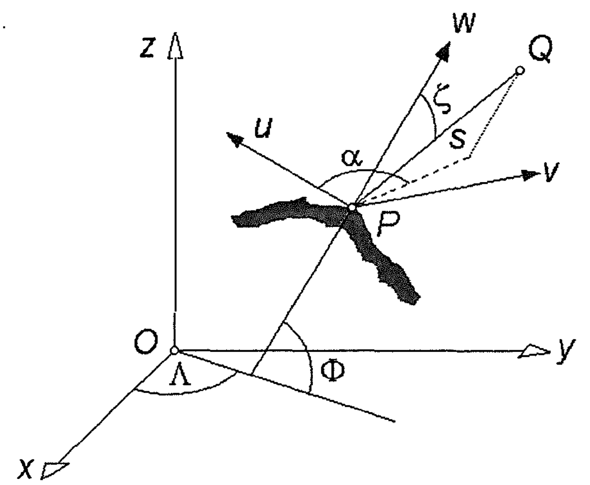

Figure 3.3

A point Q can be fixed relative to P by observing the distance s, the geodetic azimuth α, and the zenith angle ζ. **Attention!** These parameters only then refer to the cartesian system as defined above, if the actually observed values of α and ζ have been corrected for deflection of the vertical. Let ξ be the north-south component of the deflection, η the west-east component and $\vartheta = \xi\cos\alpha + \eta\sin\alpha$ the component in the direction of α. Then the reduction of the actually observed values of the zenith angle ξ^* and azimuth α^* to the geodetic values reads:

$$\xi = \xi^* \pm \vartheta, \quad \alpha = \alpha^* - \eta\cdot\tan\Phi. \tag{3.8}$$

With s, α, ζ given, the vector PQ = **s** is known:

$$\mathbf{s} = \begin{pmatrix} u \\ v \\ w \end{pmatrix} = s\begin{pmatrix} \cos\alpha\sin\zeta \\ \sin\alpha\sin\zeta \\ \cos\zeta \end{pmatrix}. \tag{3.9}$$

Now vector **s** has to be transferred into the difference vector **S** of the cartesian system of the reference ellipsoid. As *Figure 3.3* shows, both cartesian systems have different orientation, so one of the mirror matrices (2.8) has to be applied. The transformation then reads:

$$\mathbf{S} = (\Delta x, \Delta y, \Delta z)^T = \mathbf{R}_w(180° - \Lambda)\cdot\mathbf{R}_v(90° - \Phi)\cdot\mathbf{S}_v\cdot\mathbf{s} = \mathbf{R}\cdot\mathbf{s}, \tag{3.10}$$

$$\text{with} \quad \mathbf{R} = \begin{pmatrix} -\sin\Phi\cos\Lambda & -\sin\Lambda & \cos\Phi\cos\Lambda \\ -\sin\Phi\sin\Lambda & \cos\Lambda & \cos\Phi\sin\Lambda \\ \cos\Phi & 0 & \sin\Phi \end{pmatrix}.$$

Sometimes the inverse transformation may be asked for. With the difference vector $\mathbf{S}=(\Delta x,\Delta y,\Delta z)^T$ given, we get:

$$\begin{aligned} s &= \sqrt{\Delta x^2 + \Delta y^2 + \Delta z^2}, \\ \alpha &= \arctan\left(\frac{-\sin\Lambda\cdot\Delta x + \cos\Lambda\cdot\Delta y}{-\sin\Phi\cos\Lambda\cdot\Delta x - \sin\Phi\sin\Lambda\cdot\Delta y + \cos\Phi\cdot\Delta z}\right), \\ \zeta &= \arccos\left[\frac{1}{s}(\cos\Phi\cos\Lambda\cdot\Delta x + \cos\Phi\sin\Lambda\cdot\Delta y + \sin\Phi\cdot\Delta z)\right]. \end{aligned} \tag{3.11}$$

In surveying procedures terrestrial observation usually are processed not in 3D-space but in the plane of a conformal map projection (see Chapter 5). A directly measured slope distances s then first has to be reduced to the surface of the reference ellipsoid. Let be H_P and H_Q the heights above the ellipsoid (*Figure 3.3*). The corresponding distance on the ellipsoid is given by:

$$d = \sqrt{\frac{s^2 - (H_P - H_Q)^2}{\left(1 + \frac{H_P}{R}\right) \cdot \left(1 + \frac{H_Q}{R}\right)}}, \tag{3.12}$$

with R being the radius of an osculating sphere which may be put to R = 6 380 000 m for mid-latitudes. In fact, d should be a curve, but its curvature is so small that its neglection amounts only to 5 mm for d = 17 km.

Of course, areas on the Earth surface also have to be reduced to the ellipsoid. This is especially important for cadastral documents. The reduction is negative on principle, i.e. terrestrial areas A always are diminished by:

(3.13) $\delta A = -2A \frac{H_m}{R}$, with H_m = mean height of A above the ellipsoid.

For H_m = 250 m, δA = - 0.8 m^2, for H_m = 2000 m, δA = - 6.3 m^2.

4 Geodetic Datum (GD)

The term 'Geodetic Datum' includes everything necessary for the definition of a geodetic system, i.e. the dimensions of the reference ellipsoid used, its position with respect to the Earth's body expressed by the seven parameters for transformation into the ITRF, and the height reference. All in all ten parameters are necessary for the definition of a GD. There are many different GDs in use all over the world. GPS navigation receivers have stored more than one hundred GDs in their memory. Some well known GDs are: The WGS84, the North American Datum 83, the Australian Datum 84, the European Referance Frame (EUREF), a.o.

4.1 The World Geodetic System 1984 (WGS84)

As mentioned before, the WGS84 consists of the cartesian system of the CTS, the level ellipsoid (MEE), and a harmonic expansion of the gravity field. Its dimensions are such that the sum of all geoidal undulations vanishes: $\sum_{Earth} N = 0$, i.e. the geoid partly runs below the ellipsoid, partly above it so that the MEE and the geoid encompass equal volumes. The numerical values of the dimensions of the level ellipsoid are:

semi major axis	flattening
a = 6 378 137.000 m (definition)	f = 1 / 298.257 222 1 = 0.003 352 81068

Still no unique global height reference exists. Its definition is quite a tricky problem and not yet clear or internationally agreed upon.

4.2 The European Reference Frame (EUREF)

All European countries, apart from Russia, the former states of Yugoslavia, Albania, and Malta, are combined in a precise geocentric reference frame. The system is very close to WGS 84 and is meant to ensure uniform digital cartographic data for all of Europe [8]. It also serves for investigations of geodynamical processes. In the beginning, this system was based on 35 SLR- and VLBI-stations resp. (SLR: satellite laser ranging, VLBI: very long base line interferometry). Now, there is a rather dense net of permanent GPS-stations all over Europe. Because of plate tectonics these stations are subject to motions of about 1.3 cm/year so that the transformation parameters between EUREF and ITRF have to be updated periodically. Hence, it is important always to state the epoch of the coordinates used in a GIS-file. The EUREF-commission also recommended the introduction of a uniform height system for all of Europe (cf. Chapter 6).

4.3 The Geodetic Systems of some European Countries

Influenced by the former Soviet Union the East European countries had adopted the ellipsoid of *Krassovskij* as a reference ellipsoid. The height system is based on socalled »Normal Heights« (cf. Chapter 6) with reference to the tide gauge in Kronstadt (Baltic Sea, near St. Petersburg). The dimensions of the *Krassovskij*-ellipsoid are:

$$a = 6\,378\,245.0 \text{ m}, \quad f = 1\,/\,298.3.$$

The Austrian, German, and the Swiss Geodetic Systems (and those of some other countries) are based on the ellipsoid of *Bessel*. The obligatory values of the two parameters of the *Bessel*-Ellipsoid were fixed in 1886 by the German Geodetic Institute in Potsdam by the logarithms of the semi-major axis a and of the first eccentricity e^2. The position of the ellipsoid with respect to the ITRF of course differs in the three countries, they also have different height systems and different transformation parameters. The dimensions of the *Bessel*-ellipsoid now in use are:

$$a = 6\,377\,397.155 \text{ m}, \quad f = 1\,/\,299.152\,812\,8.$$

4.4 The Austrian Datum MGI

The datum of the ordinary Austrian geodetic system was established at the end of the 19th century by the Military Geographical Institute (MGI). Its Fundamental Point is the *Habsburg*-tower on mount *Hermannskogel* near Vienna. The positioning of the reference ellipsoid of *Bessel* with respect to the Earth body was achieved by interpreting the astronomical latitude and longitude of the fundamental point and the astronomical azimuth to mount *Hundsheim* as ellipsoidal values (i.e. the deflection of the vertical was put to zero and the semi-minor axis of the ellipsoid thus made to become parallel to the Earth rotational axis). In addition, the relative geoidal undulation N of mount *Hermannskogel* also was equalled to zero, i.e. the reference ellipsoid and the geoid intersect along a line through the fundamental point. Hence, the relative geoidal undulations in Austria vary between about – 2m and + 3m; the absolute ones with reference to the MEE amount to about + 45 m. In the last decades the Austrian triangulation net was part of the European ReTrig. Several satellite campaignes (DÖDOC, AGREF, AREF-1) since gave the basis for a consolidation of the Austrian system and its conversion to EUREF now is in progress. Approximate transformation parameters have already been given in Chapter 3. Austrian maps are based on the Transverse Mercator Projection (*Gauß-Krüger*) and on *Lambert*'s Conformal Conic Projection with two Isometric Parallels (see Chapter 5). It is important to note that for practical an historical reasons in the ordinary Austrian system MGI geodetic longitude is reckoned not from *Greenwich* but from *Ferro* (span. *Hierro*, i.e. the westernmost of the Canarian Islands). On the island itself there is no fixpoint marking the zero meridian, *Ferro* serves only as the ideal concept of a meridian exactly 20° west of the Astronomical Observatory of Paris. In order to convert *Ferro*-longitudes to *Greenwich* the relation holds:

$$\Lambda_{Gr} = \Lambda_F - 17°40'\,00'' \text{ exactly.}$$

The Austrian common **height system** also originated in the 19th century. Its reference point is a benchmark on the customs bureau on the *Molo Sartorio* in *Trieste*. The system can be called „quasi-orthometric" (see Chapter 6 on height systems). Austria has a modern geopotential levelling net (i.e. in combination with gravity measurements) as part of the European levelling system but not yet in common usage. The conversion of the ordinary heights to strictly orthometric ones with reference to the European horizon (see Chapter 6) is in progress.

4.5 The German System

The common German geodetic system was established in a similar way as the Austrian one but with the Fundamental Point *Rauenberg* near Potsdam and the astronomical azimuth *Rauenberg* → *Marienkirche* (Berlin). It is represented by the „Deutsches Hauptdreiecksnetz" DHDN (German Primary Triangulation Net). The transformation parameters DHDN → ITRF are (no warrant given):

Translation vector	rotation angles	scale factor
$\delta x = 583$ m,	$\omega_x = 0''$,	$m = 11.1$ ppm (mm per km).
$\delta y = 68$ m,	$\omega_y = 0''$,	
$\delta z = 395$ m,	$\omega_z = 3.4''$,	

As in Austria, satellite campaigns furnished ITRF-coordinates for many fixpoints. The German maps are based on the Transverse Mercator Projection (*Gauß-Krüger*).

Till some years ago the **German height system** was represented by the „Deutsches Haupthöhennetz DHHN (German First Order Levelling Net). Since 1879 the height reference was per definition the benchmark on the old Berlin Astronomical Observatory with an assumed height of 37.000 m above sealevel. This reference was called „Normal Null" *NN* (normal null). Since recently the German height system as part of the European levelling net has been converted to Normal Heights (see Chapter 6).

Here, some exemplary calculations may be helpful. Just to demonstrate the calculating procedures the data are assumed to be exact which in reality is not the case.

- Example #1. Given: fictitious cartesian coordinates in the ITRF. Wanted: ellipsoidal coordinates for WGS84.

$$\begin{pmatrix} x \\ y \\ z \end{pmatrix}_{\mathrm{ITRF}} = \begin{pmatrix} 4\,278\,160.287\ \mathrm{m} \\ 831\,590.119\ \mathrm{m} \\ 4\,642\,349.872\ \mathrm{m} \end{pmatrix}_{\mathrm{ITRF}} . \tag{Ex 1.1}$$

Applying formulae (3.4, 3.5, 3.6) we get:

$$\begin{pmatrix} \Phi \\ \Lambda \\ H \end{pmatrix}_{\mathrm{WGS}} = \begin{pmatrix} 47°00'00.0000'' \\ 11°00'00.0000'' \\ 800.000\ \mathrm{m} \end{pmatrix}_{\mathrm{WGS}} . \tag{Ex 1.2}$$

Inverse transformation with (3.3) leads exactly to (Ex 1.1).

- Example #2. 7-parameter transformation into another geodetic datum. We take the values of the parameters as stated above (ITRF $\rightarrow$ MGI). Just to give the reader the opportunity to check his own calculations the shift vector is assumed to be exact to the millimeter. Evaluation of (2.6) results in:

$$\begin{pmatrix} x \\ y \\ z \end{pmatrix}_{\mathrm{MGI}} = \begin{pmatrix} 4\,277\,559.545\ \mathrm{m} \\ 831\,501.971\ \mathrm{m} \\ 4\,641\,884.890\ \mathrm{m} \end{pmatrix}_{\mathrm{MGI}} . \tag{Ex 2.1}$$

Two facts need special attention. First, we assumed the transformation parameters to be exact just for the demonstration. But in reality they were good only for an accuracy of 2 - 3 m. Now suppose the ITRF-coordinates (Ex 1.1) had cm-accuracy (obtained from a GPS-campaigne), then this accuracy would be lost by the transformation. Second, the inverse transformation (by inverting the signs of the transformation parameters) is incorrect by 3 mm in x, 4 mm in y, and by 1 mm in z. That's due to the use of the simplified rotation matrix (2.7).

- Example #3. Given point P in datum ITRF by (Ex 1.1.) and terrestrial measurements of s, α, ζ to point Q. Wanted: the difference vector **S** and the coordinates of Q in ITRF.

$$\begin{pmatrix} s \\ \alpha \\ \zeta \end{pmatrix} = \begin{pmatrix} 650.000\ \mathrm{m} \\ 55°00'00'' \\ 83°00'00'' \end{pmatrix} . \tag{Ex 3.1}$$

Using (3.8) we get:

$$\mathbf{s} = \begin{pmatrix} u \\ v \\ w \end{pmatrix}_Q = \begin{pmatrix} 370.046\ \mathrm{m} \\ 528.480\ \mathrm{m} \\ 79.215\ \mathrm{m} \end{pmatrix}_Q . \tag{Ex 3.2}$$

The transformation matrix, with Φ, Λ taken from (Ex 1.2), becomes:

$$\mathbf{R} = \begin{pmatrix} -0.717916674 & -0.190808995 & 0.669468000 \\ -0.139548865 & 0.981627183 & 0.130131422 \\ 0.681998360 & 0 & 0.73135370 \end{pmatrix}. \qquad \text{(Ex 3.3)}$$

A good check of the calculation is to test for $\det|\mathbf{R}| = -1$ (negative sign because of the mirror matrix). Multiplication of **R** and (Ex 3.2) gives the difference vector **S** and the coordinates of point *Q* in the ITRF:

$$\begin{pmatrix} \Delta x \\ \Delta y \\ \Delta z \end{pmatrix} = \begin{pmatrix} -313.469\,\text{m} \\ 477.439\,\text{m} \\ 310.304\,\text{m} \end{pmatrix}, \quad \begin{pmatrix} x \\ y \\ z \end{pmatrix}_Q = \begin{pmatrix} x \\ y \\ z \end{pmatrix}_P + \begin{pmatrix} \Delta x \\ \Delta y \\ \Delta z \end{pmatrix} = \begin{pmatrix} 4\,277\,846.818\,\text{m} \\ 832\,067.558\,\text{m} \\ 4\,642\,660.176\,\text{m} \end{pmatrix}_Q. \qquad \text{(Ex 3.4)}$$

Inverse solution, i.e. calculation of s, α, ζ from u, v, w renders the original values exactly.

5 Isothermal Coordinates and Conformal Mapping (Grid Systems)

Surveying, cartography, and GIS require plane coordinates. Thus, the ellipsoid has to be mapped onto the plane. This can be done in many different ways. It is not possible to map the ellipsoid or the sphere onto the plane without distortions of distances [9]. But there are map projections which either give a correct representation of areas (equal area, or equivalent also authalic or homalographic projections) or of angles (conformal or orthomorphic projections) in the plane. There is a great variety of small-scale world maps by projections of the sphere [10], many of them being equivalent. In geodesy and surveying conformal maps are preferred. Not that the preservation of angles is of such importance nowadays, but as distortions cannot be avoided, at least they should be independent of directions.

A conformal mapping between two surfaces is achieved if an 'isothermal' net of parameter lines of one surface is brought into a one-to-one correspondance to an isothermal net of the other one. 'Isothermal' means that the parameter lines are orthogonal and isometric (of same scale). In other words, the nets have to consist of infinitesimal squares. The plane cartesian coordinate system is isothermal, the net of meridians (Λ = const.) and parallels (Φ = const.) of the ellipsoid is not. It is orthogonal, but not isometric (cf. *Figure 5.1a*). In order to obtain an isothermal net, all we have to do is to change the density of parallels so that the net becomes isometric (*Figure 5.1b*; of course, the nets of parameter lines extend up to the pole but for graphical reasons the polar regions are omitted).

The isothermal net is achieved by introducing the 'isometric latitude' q as function of the ellipsoidal latitude Φ (*Mercator*-function):

$$\text{(5.1)} \qquad q = \ln\left[\tan\left(\frac{\pi}{4} + \frac{\Phi}{2}\right) \cdot \left(\frac{1 - e\sin\Phi}{1 + e\sin\Phi}\right)^{e/2}\right].$$

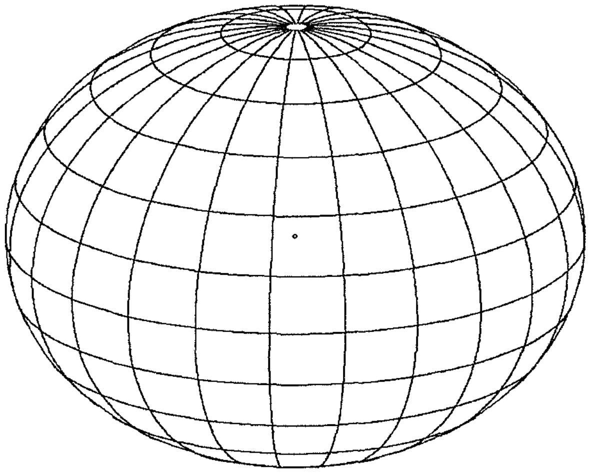

Figure 5.1a: Geodetic net of meridians and parallels

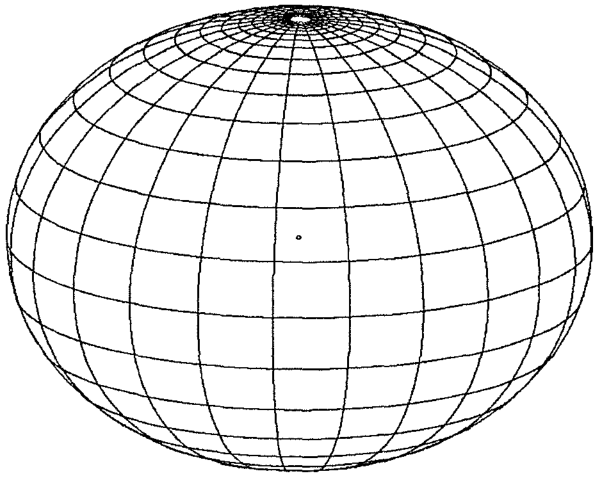

Figure 5.1b: Isothermal net

Note that e is the first excentricity of the ellipsoid and **not** the base of the natural logarithm! The inversion of (5.1) is done by iteration:

$$(5.1a) \qquad \Phi = 2\arctan[k \cdot \exp(q)] - \pi/2, \quad \text{where} \quad k = \left(\frac{1+e\sin\Phi}{1-e\sin\Phi}\right)^{e/2}.$$

With $k = 1$ as starting value, Φ results correctly after a few iterations. Now, all possible conformal mappings onto the *xy*-plane result from the solution of the *Cauchy-Riemann* differential equations in form of a complex analytical (holomorphic) function:

$$(5.2) \qquad x + i \cdot y = f(q + i \cdot \Lambda), \qquad i = \sqrt{-1}.$$

The x-coordinate of the plane system is the real part of (5.2), the y-coordinate the imaginary part. Here it is important to note that the geodetic plane coordinate system is mathematically negative, i.e. the x-axis points to north, the y-axis to east.

There is no best projection. But some are better suited for geodetic purposes than others. From the variety of conformal maps of the ellipoid only the most important ones are dealt with here.

5.1 The Meridian Strip Projection (Transverse Mercator Projection)

This projection originally was derived by *Gauss*. The formulae for practical calculations were developed by various geodesists in different countries. Hence, this projection is known under several names: In Central Europe as '*Gauss-Krüger*-Projection', in Italy as '*Gauss-Boaga*-Projection', etc. The internationally accepted name is 'Transverse Mercator-Projection' (TMP). A particular meridian of the ellipsoid with longitude Λ_0 is adopted as central meridian (CM) of the projection. Principally this could be any meridian, but usually only those are taken with longitudes divisible by 3, like 6°, 9°, 12°, a.s.o. A small zone $\pm\,\Delta\Lambda$ east and west of the CM then is mapped by equation (5.2) in such a way that the CM is represented on the plane without distortion, i.e. in its true length. The projection of the CM becomes the *x*-axis, that of the equator the *y*-axis (*Figure 5.2a*).

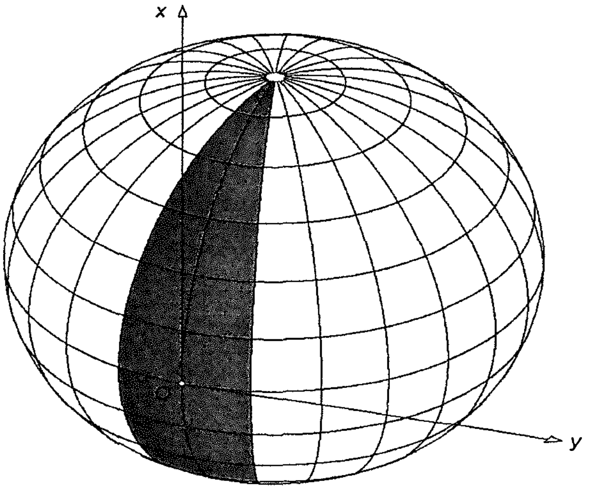

Figure 5.2a

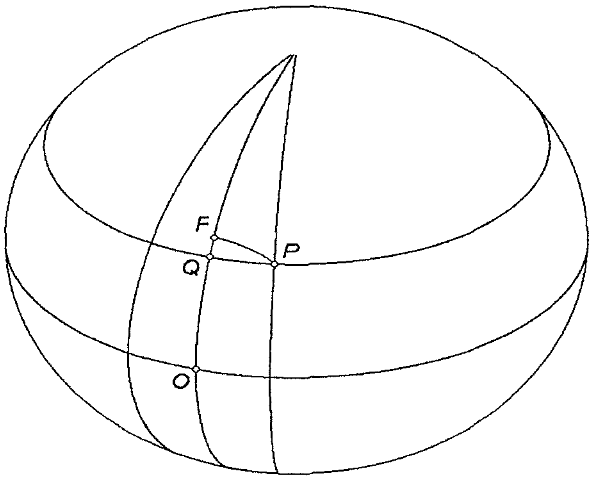

Figure 5.2b

The origin of the plane coordinate system thus is the intersection of the CM with the equator of the reference ellipsoid in its special position. Note that in Cartography and Photogrammetry the plane coordinate system frequently is defined with the *x*-axis pointing to the East, the *y*-axis to North. The total extension in longitude is 3° ($\Delta\Lambda = \pm$ 1.5°), in some countries like the Asian parts of the former USSR or China, it is 6°. Areas of the ellipsoid adjacent to the 3°-zone must be mapped on the next strip with a new CM. It should be stressed that it is impossible to obtain rigorous formulae for the TMP, but only approximate ones. Contrary to widespread opinions the TMP is not restricted to small zones and it can even be extended across the poles. However, this needs advanced mathematics beyond the scope of this treatise. The distortions increase rapidly with the distance from the CM as can be seen in *Figure 5.3* which shows a large part of the world in the TMP with CM through Greenwich (look at South America).

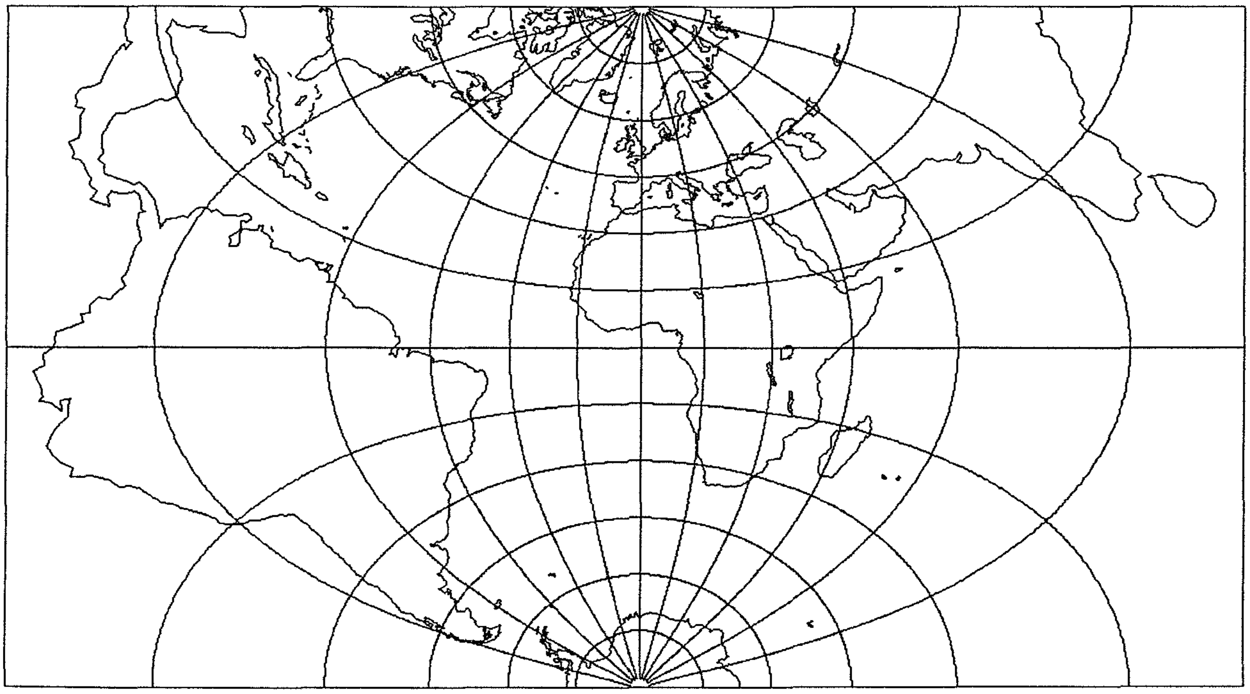

Figure 5.3

When TMP is applied to small zones simple but cumbersome formulae can be obtained by a *Taylor*-expansion of (5.2). These practical formulae cannot be extended beyond a 6°-zone without loss of accuracy, and they also fail near the poles. For 3°-zones more compact formulae exist which are given below [11]. Up to ± 1.5° distance from the CM these formulae are correct to 1 – 2 mm. The following equations are generally valid, but the numerical values of the coefficients depend on the reference ellipsoid used. First compute the constants:

$$
\begin{aligned}
\alpha &= a\left(1-e^2\right)\frac{\pi}{180}\left(1+\tfrac{3}{4}e^2+\tfrac{45}{64}e^4+\tfrac{175}{256}e^6+\tfrac{11025}{16384}e^8\right),\\
\beta &= \tfrac{1}{2}a\left(1-e^2\right)\cdot\left(\tfrac{3}{4}e^2+\tfrac{15}{16}e^4+\tfrac{525}{512}e^6+\tfrac{2205}{2048}e^8\right),\\
\gamma &= \tfrac{1}{4}a\left(1-e^2\right)\cdot\left(\tfrac{15}{64}e^4+\tfrac{105}{256}e^6+\tfrac{2205}{4096}e^8\right),\\
\delta &= \tfrac{1}{6}a\left(1-e^2\right)\cdot\left(\tfrac{35}{512}e^6+\tfrac{315}{2048}e^8\right).
\end{aligned}
\tag{5.3}
$$

In most of the formulas use is made of a particular point on the central meridian, the foot-point F (*Figure 5.2b*). It is the intersection of the CM with the geodetic line through a point P perpenticular to the CM. Its latitude always is somewhat higher than that of point Q an the parallel circle. The peculiarities of the TMP are such that P and F have different latitudes but equal x-coordinates.

Given a point $P(\Phi, \Delta\Lambda=\Lambda-\Lambda_0)$. Now compute Φ_F and the auxiliary quantitiy V_F:

$$
\begin{aligned}
&V=\sqrt{1+e'^2\cos^2\Phi}, \quad \Phi_F=\arctan\left[\frac{\tan\Phi}{\cos(\Delta\Lambda\cdot V)}\right],\\
&V_F=\sqrt{1+e'^2\cos^2\Phi_F}, \quad p=\frac{1}{V_F}\tan\Delta\Lambda\cos\Phi_F.
\end{aligned}
\tag{5.4}
$$

The plane coordinates x, y then are:

$$
\begin{aligned}
&x=\alpha\cdot\Phi_F-\beta\sin 2\Phi_F+\gamma\cdot\sin 4\Phi_F-\delta\sin 6\Phi_F,\\
&y=c\cdot\ln\left(p+\sqrt{1+p^2}\right), \quad c=a^2/b.
\end{aligned}
\tag{5.5}
$$

The coefficient α has the dimension meters per degree (m/°), so that in the first term of x, Φ_F has to be introduced in degrees. All other coefficients are in meters. Up to ± 1.5° distance from the CM these formulae are correct to 1 – 2 millimeters. The plane orthogonal x,y-net forms what is called the 'grid system'.

The inverse problem is the computation of Φ, Λ from x, y. First we compute some coefficients in function of the flattening:

$$
n=\frac{f}{2-f}, \quad \zeta=\frac{270}{\pi}\left(n-\tfrac{9}{16}n^3\right) \quad \eta=\frac{945}{4\pi}n^2, \quad \vartheta=\frac{2265}{8\pi}n^3. \tag{5.6}
$$

Now the latitude of point F can be computed from the given coordinate x by:

(5.7) $$\Phi_F = \psi + \zeta \sin 2\psi + \eta \sin 4\psi + \vartheta \sin 6\psi \quad \text{with} \quad \psi = \frac{x}{\alpha}.$$

$\Delta\Lambda$ and Φ then result from:

(5.8)
$$\lambda = \left|\frac{y}{c}\right|, \quad \Delta\Lambda = \arctan\left\{\frac{V_F}{2\cos\Phi_F}\left[\exp(\lambda) - \exp(-\lambda)\right]\right\} \cdot \mathrm{SGN}(y),$$
$$\Phi = \arctan\left[\tan\Phi_F \cos(V_F \cdot \Delta\Lambda)\right], \quad \Lambda = \Lambda_0 + \Delta\Lambda.$$

We give the numerical values of the coefficients for two ellipsoids, for that of the WGS84 and for the *Bessel*-ellipsoid.

Parameter	*Bessel*-ellipsoid	WGS 84-ellipsoid
a	6 377 397.155 m	6 378 137.000 m
f	0.003 342 773 18	0.003 352 810 68
E^2	0.006 674 372 2	0.006 694 380 0
c	6 398 786.848 m	6 399 593.626 m
α	111 120.619 6 m/°	111 132.952 5 m/°
β	15 988.638 5 m	16 038.508 6 m
γ	16.729 9 m	16.832 6 m
δ	0.021 8 m	0,022 0 m
ζ	0.143 885 358°	0.144 318 133°
η	0.000 210 780°	0.000 212 050°
ϑ	0.000 000 423°	0.000 000 427°

Note! In many countries a constant factor is added to the y-coordinate in order to avoid negative signs and to indicate the zone. Frequently, these coordinates are then termed '*Right*' for y, and '*High*' for x. As an example the Austrian system may be explained. The Austrian territory is covered by three *Gauss-Krüger* strips each of 3° width and the CMs in 28°, 31°, 34° east of *Ferro.* In order to support environmental planning and rescue actions the socalled "Federal Alert System" (Bundesmeldentz) was introduced in 1983. To avoid negative signs of the y-coordinates and to characterize the strip a constant number is added to the relevant y-coordinate. The new coordinate then is called *Right*:

for CM 28°: $R = y + 150\,000$ m,
for CM 31°: $R = y + 450\,000$ m,
for CM 34°: $R = y + 750\,000$ m.

As the whole of the Austrian territory lies within the range of six million meters distance from the equator, the digit 6 in the x-coordinate is omitted and the new coordinate called *High*: E.g. a point in the strip CM 31° with the coordinates x = 6 377 849.351 m, y = – 43 088.417 m thus becomes R = 406 911.583 m, H = 377 849.351 m.

For higher demands on accuracy and for greater distances from the CM the best practical formulas are those given by *Krüger* [12]. They are simple enough so that they may be evaluated on a good pocket computer, but nevertheless are accurate to the millimeter even for large distances from the CM. These formulas are remarcable because of their symmetrical construction. The fact that *Krüger* made extensive use of hyperbolic functions handicapped the widespread usage before the advent of personal computer. To emphasize the hyperbolic functions, in the following they are written in capital letters. E.g. ATANH stands for area tan hyp, i.e. the inverse function of TANH.

First compute and store the ellipsoidal constants:

$$n=\frac{1-\sqrt{1-e^2}}{1+\sqrt{1-e^2}},\quad A=\frac{a}{(1+n)}\left(1+\frac{n^2}{4}+\frac{n^4}{64}\right) \tag{5.9a}$$

$$\begin{aligned}\beta_1 &= \frac{n}{2}-\frac{2}{3}n^2+\frac{37}{96}n^3-\frac{1}{360}n^4,\\ \beta_2 &= \frac{1}{48}n^2+\frac{1}{15}n^3-\frac{437}{1440}n^4,\\ \beta_3 &= \frac{17}{480}n^3-\frac{37}{840}n^4.\end{aligned} \tag{5.9b}$$

$$\begin{aligned}\gamma_1 &= \frac{n}{2}-\frac{2}{3}n^2+\frac{5}{16}n^3+\frac{41}{180}n^4,\\ \gamma_2 &= \frac{13}{48}n^2-\frac{3}{5}n^3+\frac{557}{1440}n^4,\\ \gamma_3 &= \frac{61}{240}n^3-\frac{103}{140}n^4.\end{aligned} \tag{5.9c}$$

$$\begin{aligned}\delta_1 &= 2n-\frac{2}{3}n^2-2n^3+\frac{116}{45}n^4,\\ \delta_2 &= \frac{7}{3}n^2-\frac{8}{5}n^3-\frac{227}{45}n^4,\\ \delta_3 &= \frac{56}{15}n^3-\frac{136}{35}n^4.\end{aligned} \tag{5.9d}$$

5.1.1 Transformation (Φ, Λ) $\rightarrow$ (x, y).

Given are the ellipsoidal latitude Φ and the distance to the CM $\Delta\Lambda$. Compute

$$k=\tan\left(\frac{\pi}{4}+\frac{\Phi}{2}\right)\cdot\left(\frac{1-e\sin\Phi}{1+e\sin\Phi}\right)^{e/2}, \tag{5.10a}$$

with e being the root of the first excentricity and *not* the base of the natural logarithm.

$$b=2\arctan(k)-\pi/2, \tag{5.10b}$$

(5.10c) $\xi = \arctan(\tan b \sec \Delta L), \quad \eta = \mathrm{ATANH}\{\sin\Delta L \cos b\}.$

Now the desired conformal coordinates follow from

$$(5.11)\quad \begin{aligned} x &= A\{\xi + \gamma_1 \sin(2\xi)\mathrm{COSH}(2\eta) + \gamma_2 \sin(4\xi)\mathrm{COSH}(4\eta) + \gamma_3 \sin(6\xi)\mathrm{COSH}(6\eta)\}, \\ y &= A\{\eta + \gamma_1 \cos(2\xi)\mathrm{SINH}(2\eta) + \gamma_2 \cos(4\xi)\mathrm{SINH}(4\eta) + \gamma_3 \cos(6\xi)\mathrm{SINH}(6\eta)\}. \end{aligned}$$

5.1.2 Inverse transformation $(x, y) \to (\Phi, \Lambda)$.

Compute the auxiliary quantities:

(5.12a) $\xi = x/A, \qquad \eta = y/A$,

and from that:

$$(5.12b)\quad \begin{aligned} \xi^* &= \xi - \beta_1 \sin(2\xi)\mathrm{COSH}(2\eta) - \beta_2 \sin(4\xi)\mathrm{COSH}(4\eta) - \beta_3 \sin(6\xi)\mathrm{COSH}(6\eta), \\ \eta^* &= \eta - \beta_1 \cos(2\xi)\mathrm{SINH}(2\eta) - \beta_2 \cos(4\xi)\mathrm{SINH}(4\eta) - \beta_3 \cos(6\xi)\mathrm{SINH}(6\eta). \end{aligned}$$

The final result then is obtained by (a numerical example will be given later):

$$(5.13a)\quad b = \arcsin\left(\frac{\sin(\xi^*)}{\mathrm{COSH}(\eta^*)}\right),$$

$$(5.13b)\quad \Phi = b + \delta_1 \sin(2b) + \delta_2 \sin(4b) + \delta_3 \sin(6b),$$

$$(5.13c)\quad \Delta\Lambda = \arctan\left(\frac{\mathrm{SINH}(\eta^*)}{\cos(\xi^*)}\right).$$

The following table gives the necessary numerical values of the constants for the ellipsoids of *Bessel* and for that of the GRS 80. Using formulas (5.9a) to (5.9d) we get:

Term	*Bessel*	GRS 80
A	6 377 397.1550 m	6 378 137.0000 m
e^2	$6.674\,372\,231 \cdot 10^{-3}$	$6.694\,380\,023 \cdot 10^{-3}$
n	$1.674\,184\,801 \cdot 10^{-3}$	$1.679\,220\,395 \cdot 10^{-3}$
A	6 366 742.5202 m	6 367 449.1458 m
γ_1	$8.352\,252\,72 \cdot 10^{-4}$	$8.377\,318\,25 \cdot 10^{-4}$
γ_2	$7.563\,05 \cdot 10^{-7}$	$7.608\,53 \cdot 10^{-7}$
γ_3	$1.187 \cdot 10^{-9}$	$1.198 \cdot 10^{-9}$
β_1	$8.352\,256\,13 \cdot 10^{-4}$	$8.377\,321\,68 \cdot 10^{-4}$
β_2	$5.870\,4 \cdot 10^{-8}$	$5.905\,9 \cdot 10^{-8}$
β_3	$1.66 \cdot 10^{-10}$	$1.67 \cdot 10^{-10}$
δ_1	$3.346\,491\,641 \cdot 10^{-3}$	$3.356\,551\,486 \cdot 10^{-3}$
δ_2	$6.532\,540 \cdot 10^{-6}$	$6.571\,873 \cdot 10^{-6}$
δ_3	$1.748\,8 \cdot 10^{-8}$	$1.764\,7 \cdot 10^{-8}$

5.2 Distortions of Distances and Areas

The conformal mapping leaves angles unchanged but distances and areas are distorted, the more so the farther from the CM. Distances and areas are enlarged by the TMP on principle. The length of a geodetic line on the ellipsoid be s, the corresponding length in the plane s', the areas be A on the ellipsoid and A' in the plane. It suffices to use an osculating sphere of radius R_m for calculating the distortions (the subscript m indicates that R_m has to be taken for mid-latitude of the region in question). Then the formulae hold:

$$s' = s + \frac{s}{6R_m^2}\left(y_1^2 + y_1 y_2 + y_2^2\right), \quad A' = A + \frac{A}{3R_m^2}\left(y_1^2 + y_1 y_2 + y_2^2\right), \quad R_m^2 = c^2/V_m^4. \tag{5.14}$$

y_1 and y_2 are the y-coordinates of the endpoints of a line or of the nearest and farthest point of an area with respect to the CM.

The following table gives an idea on the amounts of distortions based on the *Bessel*-ellipsoid and computed for a length of 1000 m and an area of 100 hectar in 48° latitude and for different distances from the CM.

Distance from CM	50 km	100 km	150 km
$\Delta s = s' - s$	0.031 m	0.123 m	0.276 m
$\Delta A = A' - A$	61 m^2	244 m^2	550 m^2

Note that when converting from *Gauss-Krüger* projection to UTM or when changing the central meridian the Δs and ΔA also change.

5.2.1 2D-Transformations

The transformation between two geodetic systems can be simplified by means of the TMP. Lets think of the conversion of the ITRF into some regional system (RS). First the common points in both systems are converted to conformal plane coordinates using identical CMs. Now the transformation can be performed in the plane with only four parameters necessary [7]. For their unique (minimum) determination two common points are sufficient. The transformation formula then reads:

$$\begin{pmatrix} x \\ y \end{pmatrix}_{\mathrm{RS}} = \begin{pmatrix} \delta x \\ \delta y \end{pmatrix} + (1+m)\cdot\begin{pmatrix} 1 & \omega \\ -\omega & 1 \end{pmatrix}\cdot\begin{pmatrix} x \\ y \end{pmatrix}_{\mathrm{ITRF}}. \tag{5.15}$$

This transformation can be recommended only if points within a small region have to be converted. The reason to be careful is that (5.10) contains a constant scale factor whereas the scale (distortion) actually varies with distance from the CM.

5.3 The Universal Transverse Mercator System (UTM)

For the International World Map the Earth is divided into 60 zones, each having a longitudinal extension of 6° (± 3°). The zones are numbered from 1 to 60 beginning with the zone between 180° and 174° w.o.Gr. progressing eastward. The CMs thus are: 177°, 171°, 165° w.o.Gr., a.s.f. The formulae for computing the plane coordinates are the same as for 3°-zones. It must be emphasized that formulae (5.5) when used for points in 3° distance from the CM may be fuzzy in the *x*- and the *y*-coordinates by a few millimeters. Therefore, formulae (5.9) to (5.13) have to be used. Other formulas based on *Taylor*-expansions of (5.2) can be found in [2], [9] or in text books on geodesy or cartography.

UTM-coordinates have an important peculiarity. For keeping distortions small, x and y are multiplied by the scale factor m = 0.9996. These new coordinates get special names:

(5.16) Grid Northing: $N = 0.9996 \cdot x$, Grid Easting: $E = 0.9996 \cdot y$.

By use of this scale factor isometry in the CM is lost, but occurs now in two curves parallel to the CM in a distance of about ± 180 km. Note that within these two curves distortions are negative, outside of them positive.

Again in order to avoid negative coordinates the constant of 10 000 000 m is added to N on the southern hemisphere, and 500 000 m to all E-values. These new coordinates get the adjective ‘False’:

(5.17) False Northing: $FN = N + 10\,000\,000$ m (for the southern hemisphere only)
False Easting: $FE = E + 500\,000$ m.

The NATO uses UTM based on the WGS84-ellipsoid for its military maps since several years and the member states of the European Union have decided to convert their national surveying systems and maps to EUREF-datum and to UTM-projection.

- Example #4. Convert the WGS84-coordinates of point P (Ex 1.2) into UTM with Λ_0 = 9° as central meridian. Formulae (5.3, 5.4, 5.5) give

$$\begin{pmatrix} x \\ y \end{pmatrix}_{\mathrm{UTM}} = \begin{pmatrix} 5\,209\,189.002\,\mathrm{m} \\ 152\,109.881\,\mathrm{m} \end{pmatrix}_{\mathrm{UTM}}, \qquad \text{(Ex 4.1)}$$

  and the reduced UTM-coordinates

$$\begin{pmatrix} N \\ E \end{pmatrix}_{\mathrm{UTM}} = \begin{pmatrix} 5\,207\,105.326\,\mathrm{m} \\ 152\,049.039\,\mathrm{m} \end{pmatrix}_{\mathrm{UTM}}. \qquad \text{(Ex 4.2)}$$

- Example #5. As a demonstration for *Krüger´s* formulas that example was chosen which *Krüger* himself solved in [12] by logarithmic computation. Given: Φ = 48°, $\Delta\Lambda$ = 8°; wanted x, y on basis of the *Bessel*-ellipsoid. For illustrating purposes the intermediary results also are given:

from (5.10a) $k = 2.5921839169$,
from (5.10b) $b = 47°.8092551995$,
from (5.10c) $\xi = 48°.0879361926$, (Ex 5.1)
$\eta = 0.0937424118$,
from (5.11) $x = 5\,348\,940.146$ m,
$y = 596724.111$ m,

in complete agreement with *Krüger's* result and accurate to the millimeter. For the inverse problem the above values of x and y are taken as initial ones:

from (5.12a) $\xi = 48°.1363419735$,
$\eta = 0.0937251833$,
from (5.12b) $\xi^* = 48°.0879361929$,
$\eta^* = 0.0937424118$, (Ex 5.2)
from (5.13a) $b = 47°.8092551999$,
from (5.13b) $\Phi = 48°00'00''.0000$,
from (5.13c) $\Delta\Lambda = 8°00'00''.0000$.

5.4 The Polar Stereographic Projection (PSP)

UTM is not extended into polar regions. There it is supplemented by the PSP which also is conformal. This is a projection onto a plane tangent to the ellipsoid in one of the poles. The origin of the plane system is the pole, the images of the meridians then are straight lines through the pole, and the parallels are concentric circles. As x-axis any of the meridians may be chosen, in *Figure 5.4a* it is the meridian $\Lambda_0 = 180°$. The projection equations are rigorous:

(5.18)
$$x = \rho\cos(\Lambda_0 - \Lambda), \quad y = \rho\sin(\Lambda_0 - \Lambda), \quad \text{with}$$
$$\rho = 2c\left(\frac{1+e}{1-e}\right)^{e/2} \cdot \tan\left(45° - \frac{\Phi}{2}\right) \cdot \left(\frac{1+e\sin\Phi}{1-e\sin\Phi}\right)^{e/2}, \quad c = \frac{a^2}{b}.$$

For the inversion of the problem (x, $y \to \Phi$, Λ) we first get easily:

(5.19)
$$\Lambda = \Lambda_0 - \arctan\left(\frac{y}{x}\right), \quad \rho = \frac{x}{\cos(\Lambda_0 - \Lambda)} = \frac{y}{\sin(\Lambda_0 - \Lambda)}.$$

Then we put $const = 2c\left(\frac{1+e}{1-e}\right)^{e/2}$ and $k = \left(\frac{1-e\sin\Phi}{1+e\sin\Phi}\right)^{e/2}$ for the iterative computation of Φ:

(5.20)
$$\Phi = 90° - 2 \cdot \arctan\left(\frac{\rho \cdot k}{const}\right), \quad \text{with } k = 1 \text{ as starting value.}$$

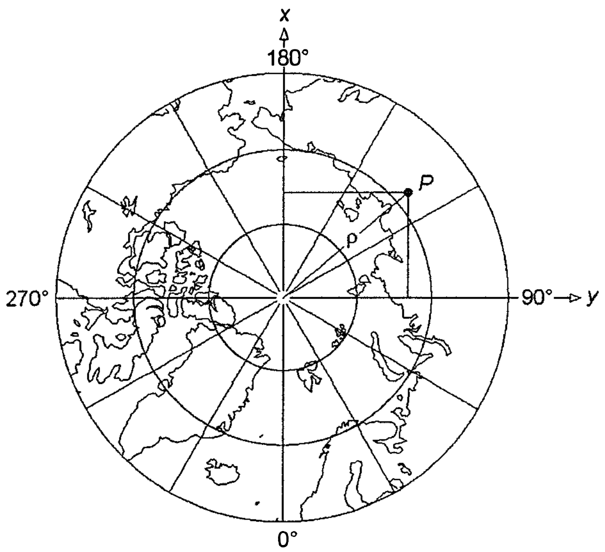

Figure 5.4a

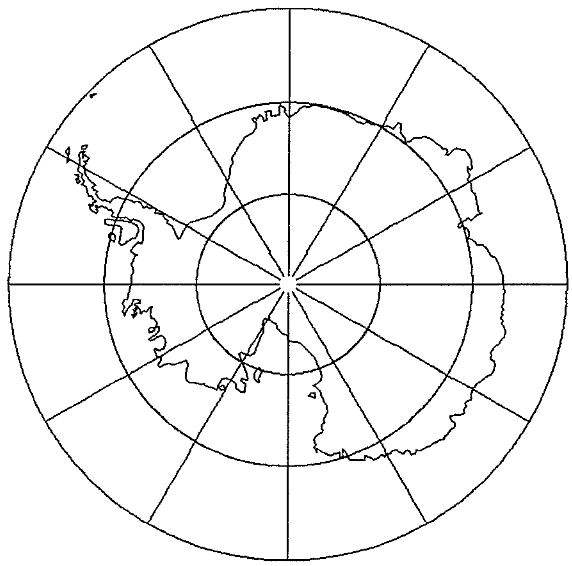

Figur 5.4b

- Example #6. Given a point in Siberia $P(\Phi = 68°$ exactly, $\Lambda = 130°$ E.o.Gr. exactly). With $\Lambda_0 = 180°$ and on basis of the WGS-ellipsoid we get from (5.13):

$$\rho = 2\,520\,283.104\text{ m},\quad \begin{pmatrix} x \\ y \end{pmatrix}_{PSP} = \begin{pmatrix} 1\,620\,006.752\text{ m} \\ 1\,930\,648.867\text{ m} \end{pmatrix}_{PSP}. \qquad \text{(Ex 6.1)}$$

Again the inverse transformation is correct.

5.5 Lambert's Conformal Conic Projection (LCC)

This extremely useful projection is the basis of the International Aeronautical Charts (Low and High Altitude Enroute Charts) and is employed in several countries (e.g. the Austrian map 1:500 000). Imagine a circular cone with its axis coinciding with the minor axis of the ellipsoid. The cone may be tangent along a parallel circle of the ellipsoid or may intersect it in two circles. These circles, of course, are mapped isometrically. When the cone is cut open along one of its generating lines and developed into the plane, the images of the meridians again are straight lines through the apex *S* of the cone (= image of the pole), and the images of the parallel circles are concentric circles. The PSP of chapter 5.4 is only a special case of the general LCC. Let the apex of the cone approach the ellipsoid until it coincides with the pole. Then the cone degenerates to a circular plane and you got the PSP.

The LCC permits to map a rather wide latitudinal zone around the whole Earth with small distortions. For conic projections it is of advantage to use polar coordinates. *Figure 5.5* shows the developed cone and the arrangement of the plane coordinates *r*, ϑ and *x*, *y*. Φ_1 and Φ_2 are the two intersecting parallels. The intersection of some CM (Λ_0) with the parallel Φ_1 may serve as origin *O* of the rectangular coordinates.

The formulae are rigorous. First compute the auxiliary quantities *n* and *A* (*q* is the isometric latitude of equation 5.1) from:

(5.21)

$$n = \frac{\ln\left(\frac{c}{V_1}\cos\Phi_1\right) - \ln\left(\frac{c}{V_2}\cos\Phi_2\right)}{q_2 - q_1},$$

$$A = \frac{c}{nV_1}\cos\Phi_1 \exp(n \cdot q_1) = \frac{c}{nV_2}\cos\Phi_2 \exp(n \cdot q_2).$$

The plane coordinates then are (5.22)

$$r = A\exp(-n \cdot q), \quad \vartheta = n \cdot (\Lambda - \Lambda_0),$$

$$x = B - r\cos\vartheta, \quad y = r\sin\vartheta, \quad B = \frac{c}{nV_1}\cos\Phi_1.$$

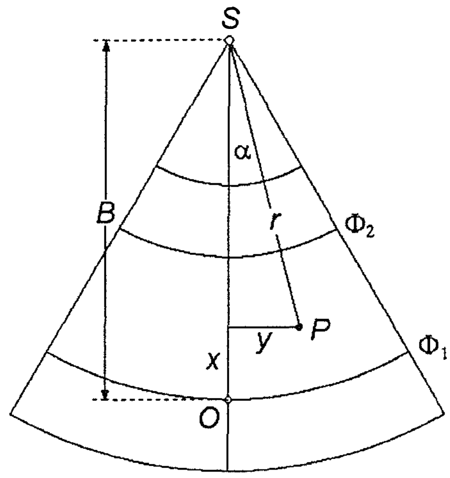

Figure 5.5

In *Figure 5.6* the zone of the world between 0° and 75° latitude is shown in LCC-projection with Φ_1 = 25° and Φ_2 = 50°.

For the inverse problem with *x*, *y*, Φ_1, Φ_2 given, first compute *n*, *A* and *B* according to (5.21) and (5.22). Then continue with ϑ, *r* and *q* from

(5.23) $$\Lambda = \frac{1}{n}\arctan\left(\frac{y}{B-x}\right) - \Lambda_0, \quad r = \frac{B-x}{\cos\vartheta} = \frac{y}{\sin\vartheta}, \quad q = \frac{1}{n}\ln\left(\frac{A}{r}\right).$$

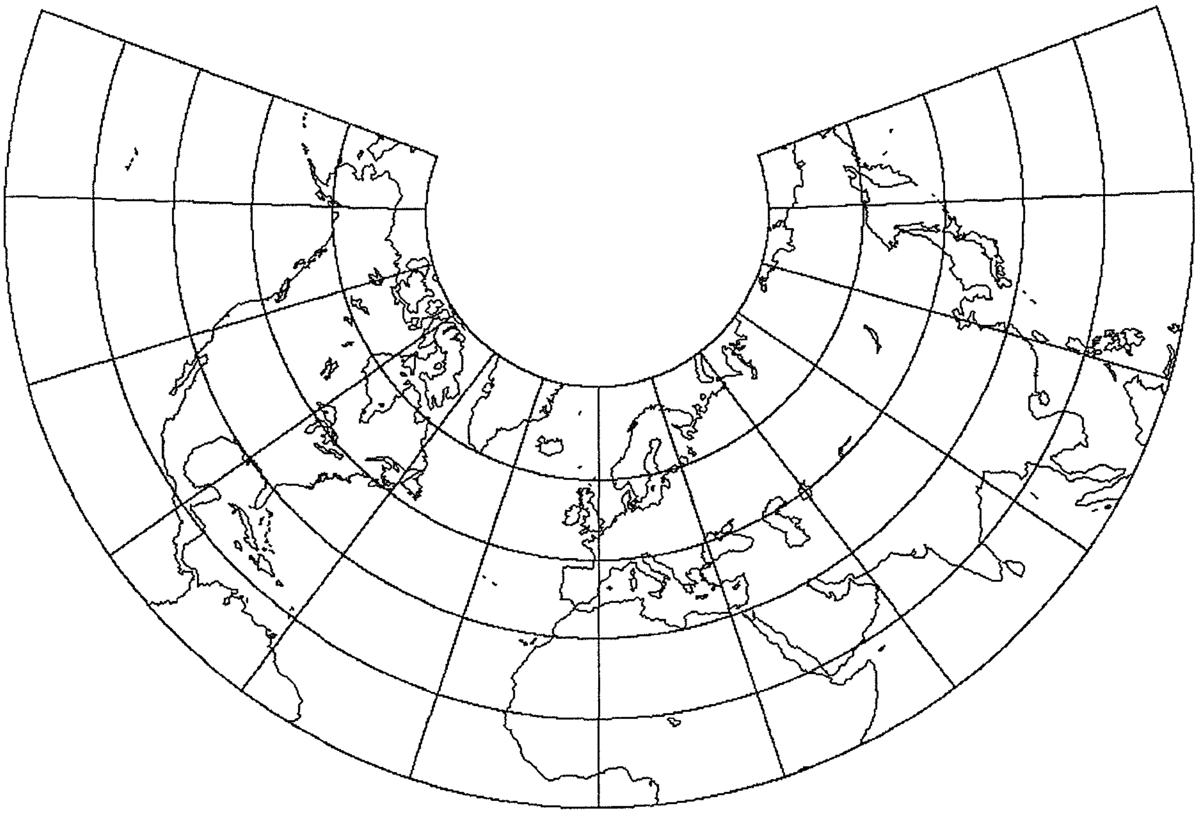

Figure 5.6

Latitude Φ then is gained by the iterating procedure (5.1a).

- Example #7. Convert point $P(\Phi = 47°, \Lambda = 11°$ E.o.Gr.) of Example #1 to LCC on basis of the WGS-ellipsoid with $\Lambda_0 = 9°$ as central meridian ($\Lambda - \Lambda_0 = 2°$), and $\Phi_1 = 25°$, $\Phi_2 = 50°$. We give all relevant values as resulting from (5.16 and 5.17).

n = 0.613 798 6271, A = 12 406 192.284 m, B = 9 423 308.980 m,
q = 0.926 729 7990, r = 7 024 262.640 m, ϑ = 1°13′39.3501″,

$$\begin{pmatrix} x \\ y \end{pmatrix}_{\text{LCC}} = \begin{pmatrix} 2\,400\,658.547\,\text{m} \\ 150\,487.625\,\text{m} \end{pmatrix}_{\text{LCC}}. \tag{Ex 7.1}$$

5.6 Conformal Double Projection (CDP)

This projection was invented by *Gauss*. The projection equations are compact and rigorous, the distortions generally quite small. The term ‘double projection’ means that the ellipsoid is conformally mapped onto a sphere, and from there onto the plane by use of the *Mercator*-function. The sphere can be defined in different ways, either circumscribing the ellipsoid along the equator (for world maps), or as an osculating sphere tangent to the ellipsoid in a well-chosen point.

The best known example for application of the CDP is Switzerland. It was introduces by *Rosenmund* in 1905, and revised by *Odermatt* 1960. First the *Bessel*-ellipsoid is conformally mapped onto the osculating sphere tangent to the ellipsoid in the astronomical observatory Bern. Then this sphere an oblique cylinder is circumscribed, contacting the sphere along the great circle perpendicular to the meridian of Bern. Now the sphere is mapped onto the cylinder (= the plane) by the simple *Mercator*-projection. The necessary formulae are the following [14].

The adopted ellipsoidal Coodinates of the fundamental point Bern are:

$$\Phi_0 = 46°57'08''.6600, \quad \Lambda_0 = 0°.$$

Let the coordinates of the osculating sphere be φ and λ and its radius according to equ. (3.7) $R = c/V_0^2$. The conformal projection of the *Bessel*-ellipsoid onto the sphere is done by:

$$\tan\left(\frac{\pi}{4}+\frac{\varphi}{2}\right) = \tan\left(\frac{\pi}{4}+\frac{\Phi}{2}\right)\left(\frac{1-e\sin\Phi}{1+e\sin\Phi}\right)^{e/2}, \quad \Delta\lambda = \Delta\Lambda, \tag{5.24}$$

with $\Delta\lambda$ = longitude difference to Bern. Now the sphere is circumscribed by a cylinder which is tangent ot the sphere along the great circle perpendicular to the meridian in Bern. The axis of the cylinder intersects the sphere in a “new” pole with its relevant sperical coordinates b, ℓ. The transformation $\varphi \to b$, $\Delta\lambda \to \ell$ is done by the sine and cosine laws of trigonometry:

$$\begin{aligned} &\cos b \sin \ell = \cos\varphi \sin\Delta\lambda, \\ &\cos b \cos \ell = \sin\varphi_0 \sin\varphi + \cos\varphi_0 \cos\varphi \cos\Delta\lambda, \\ &\sin b = \cos\varphi_0 \sin\varphi - \sin\varphi_0 \cos\varphi \cos\Delta\lambda. \end{aligned} \tag{5.25}$$

With these new coordinates the conformal mapping of the sphere onto the cylinder and thus onto the plane is gained by the simple *Mercator*-projection:

(5.26) $$x = R \ln \tan\left(\frac{\pi}{4} + \frac{b}{2}\right), \quad y = R\ell .$$

6 The Problem of Heights in Geodesy

The term 'height' can be interpreted in different ways. Even experts do not agree which height is best. Ellipsoidal heights are defined in a purely geometric way and cannot be used for technical purposes. In geodesy heights are not measured in meters but in potential differences. The potential difference $W_B - W_A$ of two points is the work do be done in order to transport the unit mass (1 kg) from *A* to *B*. This work is independent of the way taken from *A* to *B*. Such potential differences are measured by a combination of geometric leveling and gravity measurements (= geopotential leveling). The physical dimensions of a potential difference are [$m^2 s^{-2}$] but anybody wants to reckon heights in meters. That is the height problem in a nutshell. There are three requirements for a good height system:

- The heights of points are to be determined uniquely and independently of the way the measurements have taken.
- The heights should possibly be free of hypothetical assumptions.
- The corrections of measured height differences (= geometric leveling) to the system adopted should be sufficiently small.

With dW = increment of potential, g = gravity, dh = single height increment (backsight minus foresight) the fundamental relation for determining a potential difference is: $dW = -g \cdot dh$. Integrating gives:

(6.1) $$W_A - W_B = \int_A^B g \cdot dh \approx \sum_A^B g \cdot \delta h .$$

Because equipotential surfaces are not parallel to each other the result of a geometric leveling alone (without gravity) depends on the way the leveling had taken. For the construction of a leveling system a zero level has to be defined. The geoid serves this purpose, and when potential differences are referred to the geoid they are called 'geopotential numbers' *C*. *C* usually is given in units of 100 $m^2 s^{-2}$ (= kGal·m) because then the geopotential number differs only by about 2% from the pertinent height. Thus, the geopotential number of point *A* in *Figure 6.1* is given by:

(6.2) $$C_A = W_0 - W_A = \int_{P_0}^{A} g \cdot dh \approx \sum_{P_0}^{A} g \cdot \delta h .$$

When performing a geopotential leveling around a closed circuit it is evident from (6.1) that $\sum_A^A g \cdot \delta h = 0$ apart from measuring errors. As in practical surveying no gravity observations are taken it is often recommended in manuals on surveying to test the measuring errors in closed loops by checking for $\sum_{A}^{A} \delta h = 0$. This holds only for small loops. In large ones (e.g. first order levelling circuits) there is a theoretical closing error given by:

$$\varepsilon = \sum_{A}^{A} g \cdot \delta h = -\sum_{A}^{A} \frac{g - g_A}{g_A} \delta h . \tag{6.3}$$

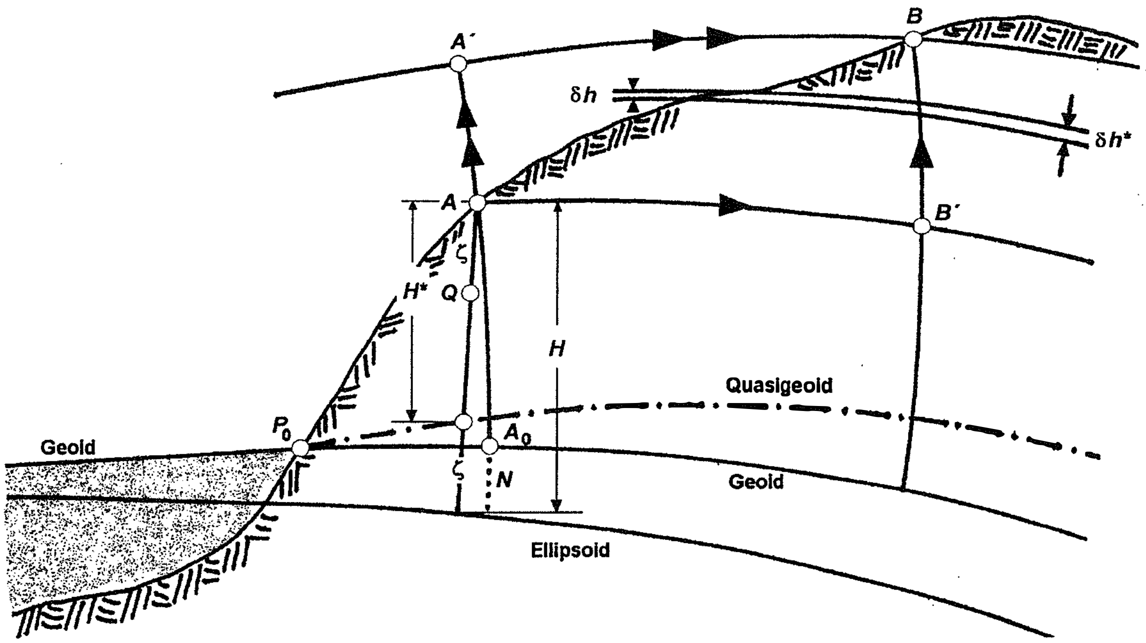

Figure 6.1, N and ζ exaggerated

Actually, national or international height systems are referred to mean sea level as observed at some coasts by tide gauges. E. g. the height reference for the East European countries is the mean sea level of the Baltic Sea measured at the tide gauge in Kronstadt near St. Petersburg. The socalled 'European Horizon' is the mean sea level of the North Sea of the years 1940 to 1958 determined by observations of the tide gauge in Amsterdam (New Amsterdam Peil NAP). However, though it was recommended that all European states should refer their height systems to the European Horizon still some countries use older systems with rather weakly defined zero levels, e.g. Austria.

6.1 Dynamic Heights (DH)

A geopotential number immediately can be converted to a quantity in meters by division through any arbitrary gravity value [m s^{-2}]. In Europe usually the theoretical gravity in 45° latitude is taken: γ_{45} = 9.806 199 m s^{-2}. The dynamic height of a point or a dynamic height difference then is given by:

(6.4) $$h_A = \frac{C_A}{\gamma_{45}}, \quad h_B - h_A = \frac{W_A - W_B}{\gamma_{45}} = \frac{1}{\gamma_{45}} \sum_A^B g \cdot dh.$$

In practical surveying nobody performs gravity measurements, so we have to convert geometric leveling results into dynamic height differences. This is achieved by the 'dynamic correction':

(6.5) $$h_B - h_A = \sum_A^B \delta h + \sum_A^B \frac{g - \gamma_{45}}{\gamma_{45}} \delta h.$$

DHs are theoretically sound and can be determined with high accuracy without any hypothetical assumption. Between two points of equal DH no water can flow. Thus DHs meet the first two requirements mentioned above but not the third one. The dynamic correction can become quite large in mountain areas. Moreover, DHs cannot be interpreted geometrically because there is no definite zero level. Hence, they cannot be combined with ellipsoidal heights obtained from GPS observations.

6.2 Orthometric Heights (OH)

The OH is the length of the slightly curved plumb line from the geoid to the Earth surface (cf. *Figure 6.1*). Thats why in German they often are called „*Meereshöhen*". Let a fictitious geopotential leveling be executed along the plumb line from A_0 to A giving the geopotential number C_A. But the same value results from a geopotential leveling along the Earth's surface as C_A is independent of path. If all quantities referring to the plumb line are characterized by an asterisk the relation holds:

(6.6) $$C_A = W_0 - W_A = \int_{A_0}^{A} g^* dh^* = h_A^* \frac{1}{h_A^*} \int_{A_0}^{A} g^* dh^* = \bar{g}_A^* h_A^* \quad \rightarrow \quad h_A^* = \frac{C_A}{\bar{g}_A^*}.$$

$\bar{g}_A^*$ is an integral mean of the gravity along the plumb line. Because we cannot measure gravity within the Earth's crust, $\bar{g}_A^*$ has to be computed from gravity values measured at the Earth´s surface. This is where hypothetical assumptions enter (density of the crust). Therefore it is hardly possible to get OHs with millimeter accuracy, and in mountain areas even the centimeters are fuzzy. From the three requirements for a good height system the first is met, the second is not, and the third much better than by dynamic heights. However, there is a drawback: Between two points with equal OH water can flow. But the most important advantage of OHs is that they can be combined with ellipsoidal heights: The difference of ellipsoidal heights equals the difference of orthometric heights plus the difference of geoidal undulations (Theorem of *Villarceau*).

(6.7) $$(H_B - H_A) = (h_B^* - h_A^*) + (N_B - N_A).$$

This can readily be taken from *Figure 6.1* if the very slight plumb line curvature is neglected.

6.3 Normal Heights (NH)

Proposed by the Russian geodesist *Molodenskij* NHs are standard in the East European countries and, since recently, also in Germany. The EUREF-commission has recommended the use of NHs for all of Europe. NHs meet all three demands for a good system. The theory is quite simple. The MEE is equipped with a theoretical gravity field. Its potential U_0 by definition is equal to the potential W_0 of the geoid. In *Figure 6.1* consider the normal to the ellipsoid through point A. In that normal a point Q must be found whose potential difference with respect to U_0 in the theoretical gravity field is equal to the potential difference of A with respect to W_0 in the real field. According to (6.2) we have:

(6.8) $$U_0 - U_Q = W_0 - W_A = C_A.$$

The NH of point A now is the distance of Q from the ellipsoid and is defined by:

(6.9) $$H_A^* = \frac{C_A}{\bar{\gamma}_Q}.$$

$\bar{\gamma}_Q$ is the integral mean of the theoretical gravity from the ellipsoid to point Q and can be computet from the gravity formula though only in an iterative way. If many points Q are determined in the manner discribed, their manifold forms a surface called ‘telluroid’ according to *Hirvonen*. The distance between the Earth´s surface and the telluroid ζ is termed ‘height anomaly’. It is not very satisfactory to measure the height of a point by a length which does not end in that point. Therefore, *Molodenskij* counted the height anomalies from the ellipsoid thus getting a new surface, the ‘quasi-geoid’. The NH now is the distance of a point on the Earth’s surface from the quasi-geoid. Note the analogy: What the geoid is for orthometric heights is the quasi-geoid for normal heights. There is also an analogous relation to the Theorem of *Villarceau*:

(6.10) $$(H_B - H_A) = (H_B^* - H_A^*) + (\zeta_B - \zeta_A).$$

The quasi-geoid is not a level surface. On the oceans it coincides per definiton with the geoid, on the continents it runs slightly above it. In the Alps the height anomalies may run up to 40 - 50 cm. The computation of height anomalies as well as of geoid undulations is a very ambitious problem. The importance of orthometric and of normal heights lies in the fact that as soon as we know the detailed geoid (or the quasi-geoid) the costly leveling operations can be substituted by GPS observations.

Finally, a comparison of the values of different heights might be instructive. They are taken from points of the Austrian first order leveling net ranging from the lowlands to the Alps. The geoid undulations N and the ellipsoidal heights H are reckond with reference to the ellipsoid of the Austrian datum MGI, **not** to EUREF.

Geopotent. Number C [kGal·m]	Dynamic Height [m]	Orthometric Height [m]	Normal Height [m]	$(\zeta - N)$ [m]	Geoid Und. N [m]	Ellipsoid. Height [m]
140.0704	142.839	142.801	142.800	+ 0.001	+ 0.60	143.40
694.0876	707.805	707.810	707.721	+ 0.089	+ 1.18	708.99
1090.1256	1111.670	1111.797	1111.645	+ 0.152	+ 2.35	1114.15
1420.8730	1448.954	1449.340	1449.037	+ 0.303	+ 2.77	1452.11

7 Satellite Navigation Systems

Chapter 7.1 will provide a brief overview about the concept and the operation of the satellite navigation systems, focusing on the well known Global Positioning System. Subsequently chapter 7.2 informs about the Russian satellite navigation system GLONASS. Moreover, the concepts of satellite based augmentation systems like WAAS and EGNOS are touched in chapter 7.3. Finally, a look forward at the upcoming European satellite navigation system GALILEO concludes chapter 7. For a more detailed information, especially concerning GPS, the reader is referred to the extensive literature in this field e.g. [7], [15].

7.1 Global Positioning System (GPS)

GPS, formally known as the NAVSTAR Global Positioning System, was initiated in 1973 to reduce the proliferation of navigation aids. By creating a system that overcame the limitations of many existing navigation systems, GPS became attractive to a broad spectrum of users worldwide. GPS has been successful in virtually all navigation applications, and because its capabilities are accessible to everybody using small, inexpensive equipment, GPS is being utilized in a wide variety of applications all over the globe. GPS is operated and maintained by the Department of Defense (DoD) of the U.S. Army.

The Global Positioning System (GPS) is a space-based radio-navigation system consisting of a constellation of satellites and a network of ground stations used for monitoring and control. A minimum of 24 GPS satellites revolve round the Earth in circular orbits at an altitude of approximately 20200 km (with a period of 12 hours sideral time, circling the earth twice a day, cf. *Fig. 2.1b*) providing users with accurate information on position, velocity, and time anywhere in the world and in all weather conditions. Currently (May 2003) 28 active GPS satellites are available. The orbital planes are tilted to the earth's equator by 55° to ensure coverage of polar regions. Powered by solar cells, the satellites continuously orient themselves to point their solar panels toward the sun and their antenna toward the Earth.

The satellites are composed of:

- **Solar Panels.** Each satellite is equipped with solar array panels. These panels capture energy from the sun providing power for the satellite throughout its life time.

- **Internal components** such as atomic clocks and radio transmitters. Each satellite contains four atomic clocks. These clocks are accurate to a nanosecond.

- **External components** such as antennas. The exterior of the GPS satellite has a variety of antennas. The signals generated by the radio transmitter are sent to GPS receivers via the L-band antennas. Another component is the radio transmitter, which generates the signal. Each satellite transmits two carrier waves L1 and L2 at the center frequencies

$$L_1: 154 \times 10{,}23 \text{ MHz} = 1575{,}42 \text{ MHz } (l_1 = 19{,}05\text{cm})$$

$$L_2: 120 \times 10{,}23 \text{ MHz} = 1227{,}60 \text{ MHz } (l_2 = 24{,}45\text{cm})$$

In order to forward information the carriers are modulated with code sequences (Pseudo Random Noise-Codes; C/A- and P-Code; see 7.2.1). An additional modulation provides the navigation message.

Currently three types of GPS satellites are in orbit: 3 **Block II**, 18 **Block II/A** (Advanced) and 7 **Block II/R** (Replenishment) satellites. The satellite categories differ mainly in functionality, state of the art electronics and last but not least in design life time which usually is limited by the life time of the on-board Rubidium and Cesium clocks as well as by the operation of the solar panels. Two satellites (PRN05, PRN06) are equipped with retroreflectors and can be tracked by Satellite Laser Ranging.Two more Block II/R satellites are scheduled for launch at the end of 2003.

In July 2004 the first **Block II/RM** (Military) is scheduled for launch. Block II/RM satellites will emit another Code signal (M-Code) at L1 which access is limited to military users. The M-Code is a substitute for SA and should ensure military advantages in accessing the GPS-system. The first **Block II/F** (Follow on) satellites should be launched in 2005, but the final schedule is not yet clear. They will offer another civil Code on L2, very similar to the current C/A-Code on L1. Another civil frequency commonly referred as L5 (1176,45 MHz) should be provided by a subsequent generation of satellites, the so-called **Block III** satellites. L5 will provide significant benefits above and beyond the capabilities of the current GPS constellation, even after the planned second civil frequency (L2) becomes available. Benefits include precision approach navigation worldwide, increased availability of precision navigation operations in certain areas of the world, and interference mitigation. Table 7.1 below summarizes operation issues and technical features of the GPS satellite categories.

Sat.-Type	Number	Launch	Design Life Time	Functionality
Block I	10	1978-1985	5 years	keine AS, SA
Block II	9	1989-1990	7.5 years	AS , SA
Block II/A	19	1990-1997	7.5 years	mutual communication capability
Block II/RM	18	1997-2006	10 years	M-Code
Block II/F	12-18	after 2005	15 years	civil code at L2
Block III	?	after 2009		civil code at L5

Table 7.1: GPS-satellite categories

GPS Control System

The operational tasks of the Control System comprise tracking of satellites in orbit, time synchronisation of the satellites to GPS time, and to calculate and upload broadcast orbit and clock information. The Control System consists of the main master control station at Colorado Springs (USA) and 5 monitor stations located at Hawaii, Kwajalein, Diego Garcia, Ascension and again Colorado Springs. It is of importance to mention again that WGS84 (World Geodetic System, Version G873) is used as reference system for GPS. The system is realized by the coordinates of the monitor stations and subsequently by the broadcast ephemeris of the GPS satellites.

7.1.1 GPS Point Positioning

GPS Point Positioning techniques are based on two observation types of varying quality. We have to distinguish between so-called Code- and Phase-measurements.

7.1.1.1 Code-Measurements

GPS satellites transmit modulations of the GPS carrier waves, the so-called C/A-Code (wavelength 300m) and the more precise P-Code (wavelength 30m). A unique code is assigned to each satellite. The C/A-Code repeats itself every millisecond while the P-Code covers a time span of 266 days. Individual weekly P-code-segments are assigned to each satellite. The P-Code may be encrypted. The receiver establishes replica of this codes and correlates the incoming satellite signal with the internal realization. The time interval necessary to shift the code replica to achieve maximum correlation between both code-segments allows for the calculation of the range between satellite and receiver.

(7.1) $$L_c = c \cdot (t_r - T_t)$$

L_c .... pseudorange
T_t .... epoch of code emmission in the satellites time frame
t_r .... reception time of Code in the receivers time frame
c .... speed of light

The Code-observation is obviously the signal´s travel time $(t_r - T_t)$ multiplied by c, which is usually superimposed by clock offsets to GPS time and therefore called 'pseudorange'. One range observation defines a sphere around the relevant satellite. As there are four unknowns, i.e. the three receiver coordinates and the clock offset, four pseudorange measurements to four different GPS satellites in view are sufficient to determine the unknowns. The satellite clock offset is part of the navigation message. Moreover, the pseudorange is affected by atmospheric delays. Thus a more extended observation equation reads:

(7.2) $$L_c = \rho + c \cdot \Delta t_u + c \cdot \Delta t_a + c \cdot \Delta t_T + c \cdot \Delta t_I + \varepsilon_R$$

ρ .... real geometric distance between receiver and satellite
Δt_u .... receiver clock offset to GPS-time
Δt_a .... satellite clock offset to GPS-time

Δt_T .... time delay due to tropospheric refraction

Δt_I .... time delay due to ionospheric refraction

ε_R .... code noise

State of the art receiver equipment allows to correlate the code segments with a resolution of 1/200 of the code wavelength or better. Thus, the noise of P-Code observations is at the ± 15 cm level, the code noise of C/A-observations is around ± 1m.

7.1.1.2 Phase Measurements

A phase observation represents the difference in phase between the emitted carrier phase f_{CR} at epoch T_t in the satellites time frame and the phase F_0 of a reference signal generated in the receiver at reception epoch t_r in the receiver time frame. This phase difference determines the remaining fractional part of the phase pseudorange but gives no information about the number of full wave cycles (ambiguities N) between satellite and receiver. To solve for these ambiguities asks for adequate measurement and processing strategies e.g. the observation duration has to be increased according to an increased baseline length. Apriori knowledge of accurate approximative coordinates also improves the ability to solve for the ambiguities.

The phase observation equation reads:

(7.3) $$L_p = \rho + c \cdot \Delta t_u + c \cdot \Delta t_a + c \cdot \Delta t_T - c \cdot \Delta t_I - c \cdot \frac{N}{f_{CR}} + \varepsilon_R$$

with

L_p .... pseudorange

$c \cdot \frac{N}{f_{CR}} = N \cdot \lambda_{CR}$ .... ambiguity times carrier wavelength

When solving correctly for the initial ambiguity *N* the phase observation represents a pseudorange measurement with extremely low measurement noise of about ± 1.5 mm or better. Because the ionosphere is a dispersive medium for the GPS radio signals here the ionospheric delay in (7.3) enters with an opposite sign. Signal propagation of the carrier is governed by the phase refractive index while code propagation is delayed according to the group refractive index.

7.1.1.3 Accuracy in Positioning

In general the accuracy of point determination with GPS depends on two factors. These are the accuracy of the pseudorange measurement and the geometry of the satellite configuration at the instant of observation. The geometry is usually described by the DOP (Dilution of Precision) number. A low number stands for a good geometry (mixture of a few high elevation with a couple of low elevation satellites) while a large DOP implies a bad geometry (e.g. urban canyon). The standard deviation of a pseudorange measurement σ_r and the standard deviation of the derived receiver position σ are linked by:

(7.4) $\sigma = DOP \cdot \sigma_r$

According to the coordinate component of interest we may distinguish between various formulations of the DOP (HDOP, VDOP, PDOP, TDOP, GDOP):

$\sigma_H = HDOP \cdot \sigma_r$ .... represents the standard deviation of the horizontal component
$\sigma_V = VDOP \cdot \sigma_r$ .... represents the standard deviation of the vertical component
$\sigma_P = PDOP \cdot \sigma_r$ .... represents the standard deviation of the 3D-position
$\sigma_T = TDOP \cdot \sigma_r$ .... represents the standard deviation of time coordinate

The $GDOP = \sqrt{(PDOP)^2 + (TDOP)^2}$ (represents the standard deviation of the 3D-position + time) and the PDOP are most popular indicators offered by almost all planning tools of GPS standard software. The DOP numbers can be calculated by a simple approximation or rigorously from the components of the covariance matrix of a code single point positiong applying the rule of error propagation. With

(7.5) $$C_{xx} = \sigma_r^2 \cdot \begin{pmatrix} q_{xx} & q_{xy} & q_{xz} & q_{xt} \\ q_{yx} & q_{yy} & q_{yz} & q_{yt} \\ q_{zx} & q_{zy} & q_{zz} & q_{zt} \\ q_{tx} & q_{ty} & q_{tz} & q_{tt} \end{pmatrix}$$ and σ_r

we obtain the standard deviation of a 3D-position by means of

(7.6) $\sigma_P = \sigma_r \sqrt{q_{xx} + q_{yy} + q_{zz}}$ which is equal to $\sigma_P = \sigma_r \cdot PDOP$

Code- and phase observations are affected by systematic as well as random errors. *Table 7.2* summarizes well known error sources and gives a realistic estimate how they contribute to the standard deviation of a C/A Code pseudorange measurement σ_r. The sources are grouped according to their origin. SA is assumed to be turned off.

	Error source	GPS [m]
Space segment	Satellite Clock	2.0
	Orbital Perturbation	1.0
	other	0.5
Control segment	Ephemeris Errors	2.5
	other	1.0
Atmosphere	Ionosphere	3.5
	Troposphere	1.5
Site	Multipath	2.5
	Receiver Noise	1.0
	other	0.5
Sum	σ_r	5.9

Table 7.2: C/A-Code Pseudorange Errors

GPS was designed to offer Precise Code Users (PPS; Precise Positioning Service) positions in real time of 22 m in the plane and 27.7 m in height at the 95% probability level (2 drms). Besides, the velocity of any moving receiver can be determined with an accuracy of at least ± 0,2 m/s [15]. The common user, on the other hand, is allowed to use only the basic SPS (Standard Positioning Service) which prohibits the use of the encryted P-Code. Before May 2000 SPS positions in addition suffered severly from Selective Availability (SA). After May 2000 the SPS accuracy approaches the PPS level. Nevertheless SPS users are still restricted to the C/A Code which is currently offered only on L1. The upcoming civil Code on L2 will allow for a proper elimination of the ionospheric delay and therefore will lead to a remarkable improvement of the SPS.

7.2 Global Navigation Satellite System (GLONASS)

GLONASS, a Satellite Navigation System developed by the Russian Federation, provides a functionality very similar to the GPS. The user is able to obtain position, velocity and timing by tracking the ranging signals of the GLONASS satellites. Both, GPS as well as GLONASS, were primarily designed as military systems which also provide civilian services with slightly degraded accuracy.

The completely deployed space segment is composed of 24 satellites regularly located in 3 orbital planes with an inclination of about 64.8 degree. The orbits of these MEO (Medium Earth Orbiter) satellites are almost circular. An orbital height of 19100km yields to a rotation period of about 11^h 15^m. The first GLONASS satellite has been launched in October 1982 but it took more than 13 years to achieve “Full Operational Capability” (FOC) in January 1996. A major problem is the short design life time of the satellites of 3.5 years. Although each launch can deliver 3 space vehicles together into their intended space location, the number of active GLONASS satellites has decreased from about 18 in 1996 to less than 8 in 2001. Currently more frequent launches, an obviously more stable funding and an upcoming new generation of space vehicles should fully restore the system in the next 5 years.

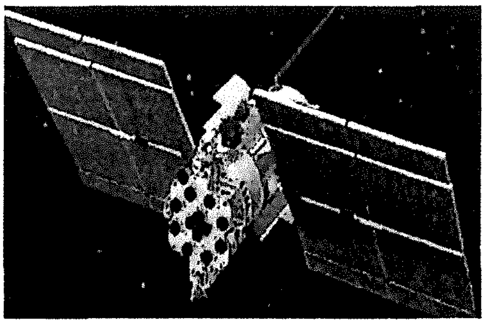

Figure 7.1: GLONASS Satellite

GLONASS-satellites transmit signals at two carriers within the L-band. But in contrast to the GPS system slightly different frequencies are assigned to the individual GLONASS satellites to discriminate between the space vehicles (Frequency Division Multiple Access). The individual center frequencies can be calculated by means of

$$L1 = 1602.0 + 0.5625\,Z \quad [\mathrm{MHz}] \quad \text{bzw.} \quad L2 = 1246.0 + 0.4375\,Z \quad [\mathrm{MHz}]$$

where Z denotes an integer number ranging from 1 to 12 (from –7 to 6 beyond 2005). GLONASS satellites provide two types of navigation signals (modulations of the carriers) which are the standard code at 0.511 MHz with a repeat cycle of 1 millisecond and the high accuracy code at 5.11MHz with a repeat cycle of 1 second.

The GLONASS broadcast ephemeris provide positions in the PZ-90 (Parametry Zemli 1990) earth-centered earth fixed reference frame. Derived geodetic coordinates refer to an ellipsoid described by the semi-major axis a= 6 378 136m and the flattening f=1/298.257839303. The quality of the PZ-90 is comparable to the WGS84 although the monitor station network is currently restricted to stations located in the Russian territory. GLONASS system time is the Russian realization of UTC (UTC(SU)) plus exactly 3 hours. The GLONASS time scale is periodically corrected for leap seconds announced by the International Earth Rotation and Reference Systems Service (IERS).

The tables below should emphasize differences and similarities between the GLONASS and the GPS system.

	GPS	GLONASS
Operating Agency	US DoD	CIS VKS
Reference System	WGS-84	PZ-90
Time System	GPS –Time (USNO)	UTC(SU) / Leap Seconds
Selective Availability	yes (till May 2000)	No
Anti-Spoofing	yes	No
FOC	July 17, 1995	January 18, 1996

Table 7.3a: Control Segment

	GPS	GLONASS
Active Satellites as of July 2003	28	9
Orbital Planes	6	3
Satellite Distribution within Plane	not regular	regular
Inclination of Planes	55°	64.8°
Orbital Height	20200 km	19100 km
Rotation Period	$11^h58.0^m$	$11^h15.7^m$
Repeat Cycle (Ground Track)	1 Sideral Day	8 Sideral Days

Table 7.3b: Space Segment

	GPS	GLONASS
Signal Division	CDMA	FDMA
Nominal Frequency	10.23 MHz	5.0 MHz
Carrier L1	1575.42 MHz	1602.0+0.5625*Z MHz
Carrier L2	1227.60 MHz	1246.0+0.4375*Z MHz
Standard Pos. Code	1.023 MHz	0.511 MHz
Precise Code	10.23 MHz	5.11 MHz
Broadcast Ephemeris	Keplerian Elements	Position and Velocity
Almanach Update	2 Hours	30 Minutes

Table 7.3c: Signal Structure

	GPS	GLONASS
Civil Navigation Service	SPS (C/A-Code)	CSA (S-Code)
Military Navigation Service	PPS (Y-Code)	CHA (P-Code)
Satellite Designation	PRN-Number	Slot-Number
Precise Ephemeris available	yes	yes
Laser Ranging	basically not	yes
Nr. of Receiver Manufacturers	many	few

Table 7.3d: Further Characteristics

7.3 Satellite Based Augmentation Systems (SBAS)

Satellite based augmentation systems were implemented to provide a level of accuracy, performance and integrity that cannot be offered by GPS or GLONASS alone. One of the major driving communities to set up SBAS was of course civil aviation but also land and maritime users require augmentations to support the performance in real time positioning. SBAS usually broadcast GPS- (GLONASS-) like navigation signals containing integrity and differential correction information by means of geostationary satellites. Up to now a few of these overlay systems are planned or will become operational in the very near future. Figure 7.2 below shows the service areas of the US-Wide Area Augmentation System (WAAS), the Canadian WAAS, the European Geostationary Navigation Overlay System (EGNOS) and the Japanese MSASystem.

Figure 7.2: SBAS service areas

7.3.1 Wide Area Augmentation System (WAAS)

The US WAAS provides a Signal-In-Space (SIS) by means of three geostationary Inmarsat satellites (GEOs), namely the POR (Pacific Ocean Region), AOR-W (Atlantic Ocean Region-West) und AOR-E (Atlantic Ocean Region-East) satellites. These satellites broadcast at the GPS-L1 frequency primarily

1. Current integrity of GPS based positions as well as integrity of signals of the remaining GEO satellites
2. Differential range corrections derived in first place from ionospheric models (more precisely from ionospheric refraction grids) and orbital error modelling

3. GEO-Ranging data to augment the number of navigation satellites available to the user.

To establish the integrity information and the range corrections WAAS uses a ground infrastructure of Wide-area Reference Stations covering the whole service area. The reference stations monitor the signals of the GPS satellites and forward the tracking data to so-called Wide-area Master Stations (WMS). At the WMS the corrections per GPS-satellite are calculated and uploaded to the GEO along with the GEO-Navigation information.

Basically WAAS should reach FOC in 2001 but due to financial and technical reasons the implemention has been delayed several times. Current estimates expect Initial Operational Capability (IOC) within the second half of year 2003. Figure 7.3 below shows the 'footprints' (areas of augmention service) of the various active geostationary satellites.

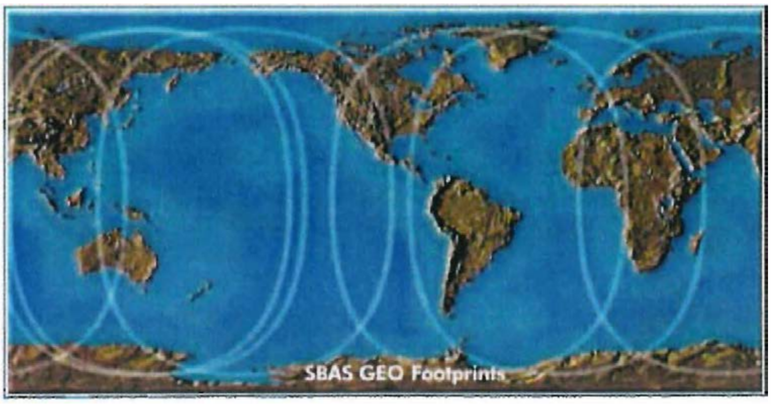

Figure 7.3: SBAS GEO footprints

Future WAAS GEOs (scheduled for launch in 2005 or later) will also provide augmentation signals at another civil frequency, namely L5. This obviously requires that L5 signals provided by a modernized GPS space segment will also become available in time. The availability of L5 will encourage developments that either can use GPS signals on both L1 and L5 to eliminate ionospheric errors or broadcasted WAAS ionospheric corrections.

7.3.2 EGNOS

Similar to WAAS the EGNOS space segment consists of three geostationary satellites comprising two Inmarsat satellites launched in 1996 and the ESA satellite ARTEMIS (Advanced Relay and Technology Mission Satellite) which was launched in 2000. From *Figure 7.3* we can deduce the service area and the fact that AOR-E (Atlantic Ocean Region - East), the most westerly GEO of EGNOS, is part of WAAS too. In the eastern region the IOR (Indian Ocean Region) satellite completes the EGNOS constellation.

Figure 7.4 shows the position of the GEOs as well as the covered service areas. The area overlaps should ensure that each user in Europe and Africa has at least two satellites simultaneously in view (in case of no local obstructions).

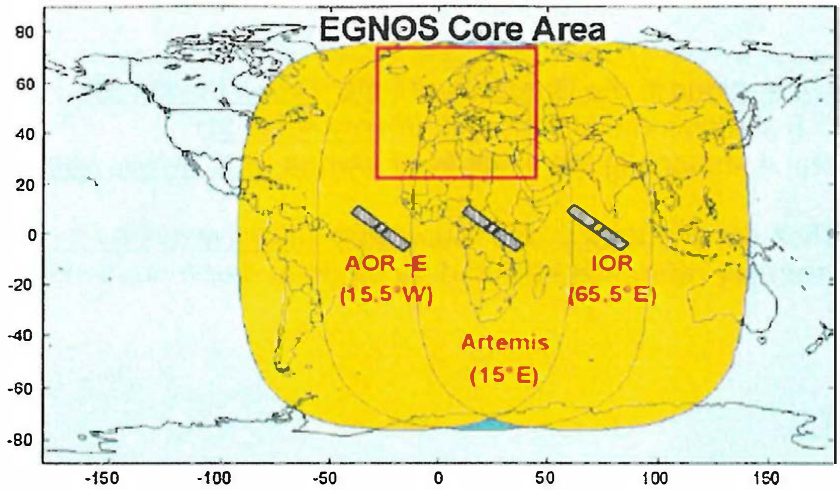

Figure 7.4: EGNOS Core Area

A complex and redundant wide area network of 34 ground reference stations and up to four control stations support EGNOS. The EGNOS messages are primarily the same as in WAAS, namely Differential Range Corrections for GPS and GLONASS, integrity information for both systems as well as for the GEOs, almanach data of the GEOs and last but not least GEO ranging data. Currently the signals are broadcasted at L1 but similar to the WAAS, future implementations may use L1 and L5.

Positioning by means of EGNOS or WAAS corrections is comparable to typical DGPS methods. The SBAS user may expect a probability of 95% that the obtained position is close to the correct position within 1.5m in the plane and within 5.0m in the vertical. These numbers might be too optimistic in case of local obstructions or additional error sources like e.g. multi-path.

The geodetic user should be aware that SBAS support typical navigation activities (aviation, car-positioning,...) by means of code range correction data and integrity information but offer no special support for precise positioning with dm or even cm accuracy. Thus high precision surveying still relies on resolving correctly the carrier phase ambiguities. Local or regional services provide the necessary phase reference data for differencing techniques or at least local ionospheric and tropospheric model parameters for high precision single point positioning.

In Germany a cooperation of the federal SAPOS-Service (http://www.sapos.de/) and the private ASCOS-Service (http://ascos.ruhrgas.de/) offers Realtime Code and Carrier Phase Correction Data for both the GPS and the GLONASS Satellite System. The data is based on a network of about 260 Reference Stations covering the whole territory of Germany. The correction data can be obtained bei means of a GSM or via the Internet.

In Switzerland the Federal Office of Topography in Berne operates a multi-purpose reference station network 'AGNES' comprising 29 reference stations. The offered services Swipos-Nav and Swipos-GIS/GEO discriminate by the targeted user groups. Swipos-Nav is a typical DGPS Service providing Code-Correction data. Swipos-GIS/GEO aims at the high-accuracy market offering reference data by means of the virtual reference station approach for all post-processing and RTK-applications.

In Austria several regions are covered by private real-time GPS/GLONASS reference station networks offering Correction Data for RTK applications via GSM or radio station.

These are:

- BEWAG: 4 stations in the Burgenland (http:///www.bewag.at)
- KELAG: 8 stations in Carinthia (http://www.kelag.at)
- Wienstrom: 4 stations in the vincinity of Vienna (http://www.wienstrom.at)

The Federal office for Metrology and Surveying (http://www.bev.gv.at) offers for the whole Austrian territory reference station data for point determination in post-processing (see [16]).

7.4 GALILEO

GALILEO, the upcoming European Satellite Navigation System, is planned to provide worldwide navigation and timing services, search and rescue services, and moreover commercial data dissemination services. The system will be to a great extent under civilian control. Currently the European Commission and the European Space Agency are close to complete the GALILEO System Definition Phase. Early in 2005 the first two test satellites should be launched to provide a preliminary signal in space. In 2006 and 2007 the bulk of operational satellites will be launched and FOC (Full Operational Capability) is scheduled for 2008.

The GALILEO space segment will consist of 30 Medium Earth Orbiting (MEO) satellites located in three orbital planes. Each plane will be inclined to the earth equator by 56° and will contain nine system plus one spare satellite in almost circular orbits. An orbital height of almost 23 620 km yields to a rotation period of about 14^h 20^m. This rotation period is not in close resonance with Earth rotation (like GPS) and therefore ensures a stable system over at least ten years without the need of frequent satellite manoeuvres. The design life time of GALILEO satellites is more than 10 years.

The GALILEO ground segment will consist, in contrast to the GPS, of more than 20 globally distributed monitor stations. The monitoring stations provide the necessary tracking data to calculate precise satellite orbit information which is sent to satellites via at least three uplink stations. The navigation information will most likely be in an extended version of keplerian elements. The GALILEO broadcast reference frame will be closely tied to the ITRF within a few cms. The navigation information will also contain the current difference between GALILEO and GPS system time. GALILEO is designed to provide a horizontal accuracy of about 4.5 m and a vertical accuracy of about 7.0 m (both at the 95% probability level). In addition GALILEO will disseminate integrity information like EGNOS and support a number of services as mentioned above.

Although GALILEO will be in principal a fully autonomous tool for satellite navigation the system design ensures as much as possible compatibility with GPS and GLONASS. The interoperability concerns for example common center frequencies at L1 and L5 or close ties of the used reference frames and timing systems. Therefore the use of future dual- or triple-system receivers will not only increase the number of trackable satellites to 50 or more but will also improve the availability, reliability and last but not least the accuracy of positioning. Thus positioning using basically Code signals of e.g. GPS + GALILEO will provide globally a horizontal accuracy of 3.5m and a vertical accuracy of about 4m (both at the 95% probability level). Also high precision positioning will certainly gain from additional signals and carriers because they allow for faster and more direct algorithms to resolve phase ambiguities.

8 References

[1] *Torge, W.*: Geodesy. Walter de Gruyter, Berlin, New York, 1991.
[2] *Heck, B.*: Rechenverfahren und Auswertemodelle der Landesvermessung. Wichmann, Karlruhe, 1987.
[3] *Bomford, G.*: Geodesy. 4^{th} ed., Clarendon Press, Oxford, 1980.
[4] *Vanicek, P., Krakiwsky, E. J.*: Geodesy: The Concept. North Holland, Amsterdam, 1986.
[5] *Hotine, M.*: Mathematical Geodesy. ESSA Monograph #2, U.S. Dep. of Commerce, Washington, D.C., 1969.
[6] *Grafarend, E.W., Kampmann, G.*: $C_{10}(3)$: The Ten Parameter Transformation in the Three-dimensional Euclidean Space. Zeitschrift für Vermessungswesen, vol. 121, 1996, p. 68-77.
[7] *Hofmann-Wellenhof, B., Lichtenegger, H., Collins, J.*: GPS - Theory and Practice. 5^{th} ed., Springer Verlag, Wien, New York, 2001.
[8] Reports of the EUREF-Commission. Veröffentlichung der Bayerischen Kommission für die Internationale Erdmessung, Heft 58, Munic, 1997.
[9] *Richardus, P., Adler, R. K.*: Map Projections. North-Holland Publishing Comp., Amsterdam, 1972.
[10] *Canters, F., Decleir, H.*: The World in Perspective. A Directory of World Map Projections. John Wiley & Sons, Chichester, England, 1989.
[11] *Bretterbauer, K.*: Die Gauss-Krüger Abbildung einfach dargestellt. Österreichische Zeitschrift für Vermessung und Geoinformation, Heft 3, 1995, p. 146 - 150.
[12] *Krüger, L.:* Konforme Abbildung des Erdellipsoides in die Ebene. Veröff. d. königl. Preussischen Geodätischen Instituts, Folge Nr. 52, Teubner, Leipzig, 1912.
[13] *Großmann, W.*: Geodätische Rechnungen und Abbildungen in der Landesvermessung. Wittwer, Stuttgart, 1976.
[14] *Kahle, H.-G.*: Einführung in die Höhere Geodäsie. Verlag der Fachvereine, Zürich, 1985.
[15] *Kaplan, E.-D.*: Understanding GPS. Principles and Applications. Artech House Publishing, Boston, 1996.
[16] *Höggerl N.,Weber R.,Pesec G.,Stangl G.,Fragner E.*: Realisierung moderner 3-D Referenzsysteme für Wissenschaft und Praxis. Österr. Zeitschrift f. Vermessung und Geoinformation, Heft 3+4, 2002, p. 92 - 108.

GEOWISSENSCHAFTLICHE MITTEILUNGEN

Bisher erschienene Bände:

Heft 1 Kolloquium der Assistenten der Studienrichtung Vermessungswesen. 1970 - 1973, Dezember 1973.

Heft 2 EGGER-PERDICH-PLACH-WAGENSOMMERER, Taschenrechner HP 45 und HP 65, Programme und Anwendungen im Vermessungswesen.
1. Auflage, März 1974, Special Edition in English, Juli 1974,
2. verbesserte Auflage, November 1974.

Heft 3 Kolloquium der Assistenten der Studienrichtung Vermessungswesen 1973 - 1974, September 1974.

Heft 4 EGGER-PALFINGER-PERDICH-PLACH-WAGENSOMMERER, Tektronix-Tischrechner TEK 31, Programmbibliothek für den Einsatz im Vermessungswesen, November 1974.

Heft 5 K.LEDERSTEGER, Die horizontale Isostasie und das isostatische Geoid, Februar 1975.

Heft 6 F.REICHART, Katalog von FK4 Horrebow-Paaren für Breiten von +30 bis +60, Oktober 1975.

Heft 7 Arbeiten aus dem Institut für Höhere Geodäsie, Wien, Dezember 1975.

Heft 8 Veröffentlichungen des Instituts für Photogrammetrie zum XIII. Internationalen Kongreß für Photogrammetrie in Helsinki 1976, Wien, Juli 1976.

Heft 9 W.PILLEWIZER, Felsdarstellung aus Orthophotos, Wien, Juni 1976.

Heft 10 PERDICH-PLACH-WAGENSOMMERER, Der Einsatz des programmierbaren Taschenrechners Texas Instruments SR-52 mit Drucker PC100 in ingenieurgeodätischen Rechentechnik, Wien, Mai 1976.

Heft 11 Kolloquium der Assistenten der Studienrichtung Vermessungswesen 1974 - 1976, November 1976.

Heft 12 Kartographische Vorträge der Geodätischen Informationstage 1976, Wien, Mai 1977.

Heft 13 Veröffentlichung des Instituts für Photogrammetrie anläßlich des 80. Geburtstages von Prof.Dr.h.c.K.Neumaier, Wien, Januar 1978.

Heft 14 L.MOLNAR, Self Checking Analytical Relative Orientation and Strip Formation, Wien, Dezember 1978.

Heft 15 Veröffentlichung des Instituts für Landesvermessung anläßlich des 80. Geburtstages von Prof.Dr.Alois Bavir, Wien, Januar 1979.

Heft 16 Kolloquium der Assistenten der Studienrichtung Vermessungswesen 1976 - 1978, Wien, November 1979.

Heft 17 E.VOZIKIS, Die photographische Differentialumbildung gekrümmter Flächen mit Beispielen aus der Architekturbildmessung, Wien, Dezember 1979.

Heft 18 Veröffentlichung des Instituts für Allgemeine Geodäsie anläßlich des 75. Geburtstages von Prof.Dipl.Ing.Dr.F.Hauer, Die Höhe des Großglockners, Wien, 1981.

Heft 19 H.KAGER, Bündeltriangulation mit indirekt beobachteten Kreiszentren, Wien, April 1981.

Heft 20 Kartrographische Vorträge der Geodätischen Informationstage 1980, Wien, Mai 1982.

Heft 21 Veröffentlichung des Instituts für Kartographie anläßlich des 70. Geburtstages von Prof.Dr.Wolfgang Pillewizer: Glaziologie und Kartographie, Wien, Dezember 1982.

Heft 22 K.TEMPFLI, Genauigkeitsschätzung digitaler Höhenmodelle mittels Spektralanalyse, Wien, Mai 1982.

Heft 23 E.CSAPLOVICS, Interpretation von Farbinfrarotbildern, Wien, November 1982.

Heft 24 J.JANSA, Rektifizierung von Multispektral-Scanneraufnahmen - Entwicklung und Erprobung eines EDV-Programms, Wien, Mai 1983.

Heft 25 Zusammenfassung der Diplomarbeiten, Dissertationen und Habilitationen an den geodätischen Instituten der TU Wien, Wien, November 1984.

Heft 26 T.WUNDERLICH, Die voraussetzungsfreie Bestimmung von Refraktionswinkeln, Wien, August 1985.

Heft 27 G.GERSTBACH (Hrsg.), Geowissenschaftliche/geotechnische Daten in Landinformationssystemen - Bedarf und Möglichkeiten in Österreich, Juni 1986.

Heft 28 K.NOVAK, Orientierung von Amateuraufnahmen ohne Paßpunkte, Wien, August 1986.

Heft 29 Veröffentlichung des Instituts für Landesvermessung und Ingenieurgeodäsie, Abt. Ingenieurgeodäsie, anläßlich des 80. Geburtstages von Prof.Dipl.Ing.Dr.F.Hauer, Wien, Oktober 1986.

Heft 30 K.-H.ROCH, Über die Bedeutung dynamisch ermittelter Parameter für die Bestimmung von Gesteins- und Gebirgseigenschaften, Wien, Februar 1987.

Heft 31 G. HE, Bildverbesserung mittels digitaler Filterung, Wien, April 1989.

Heft 32 F.SCHLÖGELHOFER, Qualitäts- und Wirtschaftlichkeitsmodelle für die Ingenieurphotogrammetrie, Wien, April 1989.

Heft 33 G.GERSTBACH (Hrsg.), Geowissenschaftliche/geotechnische Daten in Landinformationssystemen - Datenbestände und Datenaustausch in Österreich, Wien, Juni 1989.

Heft 34 F.HOCHSTÖGER, Ein Beitrag zur Anwendung und Visualisierung digitaler Geländemodelle, Wien, Dezember 1989.

Heft 35 R.WEBER, Lokale Schwerefeldmodellierung unter Berücksichtigung spektraler Methoden zur Geländereduktion, Wien, April 1990.

Heft 36 o.Prof.Dr.Hans Schmid zum 70. Geburtstag. Veröffentlichung der Abteilung für Landesvermessung, Wien, Oktober 1990.

Heft 37 G.GERSTBACH, H.P.HÖLLRIEGL und R.WEBER, Geowissenschaftliche Informationsbörse - Eine Nachlese zu GeoLIS II, Wien, Oktober 1990.

Heft 38 R.ECKER, Rastergraphische Visualisierungen mittels digitaler Geländemodelle, Wien, August 1991.

Heft 39 Kartographische Forschungen und Anwendungsorientierte Entwicklungen, herausgegeben von W.Stams und F.Kelnhofer zum 80. Geburtstag von Prof.Dr.W.Pillewizer, Wien, Juli 1991.

Heft 39a W.RIEGER, Hydrologische Anwendungen des digitalen Geländemodelles, Wien, Juli 1992.

Heft 40 K.STEINNOCHER, Methodische Erweiterungen der Landnutzungsklassifikation und Implementierung auf einem Transputernetzwerk, Wien, Juli 1994.

Heft 41 G.FORKERT, Die Lösung photogrammetrischer Orientierungs- und Rekonstruktionsaufgaben mittels allgemeiner kurvenförmiger Elemente, Wien, Juli 1994.

Heft 42 M.SCHÖNER, W.SCHÖNER, Photogrammetrische und glaziologische Untersuchungen am Gàsbre (Ergebnisse der Spitzbergenexpedition 1991), Wien, Mai 1996.

Heft 43 M.ROIC. Erfassung von nicht signalisierten 3D-Strukturen mit Videotheodoliten, Wien, April 1996.

Heft 44 G.RETSCHER, 3D-Gleiserfassung mit einem Multisensorsystem und linearen Filterverfahren, Wien, April 1996.

Heft 45 W.DAXINGER, Astrogravimetrische Geoidbestimmung für Ingenieurprojekte, Wien, Juli 1996.

Heft 46 M.PLONER, CCD-Astrometrie von Objekten des geostationären Ringes, Wien, November 1996.

Heft 47 Zum Gedenken an Karl Killian "Ingenieur" und "Geodät" 1903 -1991, Veröffentlichung der Fachgruppe Geowissenschaften, Wien, Februar 1997.

Heft 48 A.SINDHUBER, Ergänzung und Fortführung eines digitalen Landschaftsmodelles mit multispektralen und hochauflösenden Fernerkundungsaufnahmen, Wien, Mai 1998.

Heft 49 W.WAGNER, Soil Moisture Retrieval from ERS Scatterometer Data, Wien, Dezember 1998.

Heft 50 R.WEBER, E.FRAGNER (Editoren), Prof. Bretterbauer, Festschrift zum 70.Geburtstag, Wien, Juli 1999.

Heft 51 Ch.ÖHRENEDER, A Similarity Measure for Global Image Matching Based on The Forward Modeling Principle, Wien, April 1999.

Heft 52 M.LECHTHALER, G.GARTNER, Per Aspera ad Astra, Festschrift für Fritz Kelnhofer zum 60. Geburtstag, Wien, Jänner 2000.

Heft 53 F.KELNHOFER, M.LECHTHALER, Interaktive Karten (Atlanten) und Multimedia – Applikationen, Wien, März 2000.

Heft 54 A.MISCHKE, Entwicklung eines Videotheodlit-Meßsystems zur automatischen Richtungsmessung von nicht signalisierten Objektpunkten, Wien, Mai 2000

Heft 55 Veröffentlichung des I.P.F. anlässlich der Emeritierung von Prof. Dr. Peter Waldhäusl, Wien.

Heft 56 F.ROTTENSTEINER, Semi-automatic Extraction of Buildings Based on Hybrid Adjustment Using 3D Surface Models and Management of Building Data in a TIS, Wien, Juni 2001.

Heft 57 D.LEGENSTEIN, Objektrekonstruktion aus perspektiven Bildern unter Einbeziehung von Umrisslinien, Wien, Mai 2001.

Heft 58 F.KELNHOFER, M.LECHTHALER und K.BRUNNER (Hrsg.), Telekartographie und Location Based Services, Wien, Jänner 2002.

Heft 59 K.BRETTERBAUER, Die runde Erde eben dargestellt; Abbildungslehre und sphärische Kartennetzentwürfe, Wien, 2002.

Heft 60 G.GARTNER, Maps and the Internet 2002, Wien, 2002.

Heft 61 L.DORFFNER, Erzeugung von qualitativ hochwertigen 3D Photomodellen für Internetbasierte Anwendungen mit besonderem Augenmerk auf Objekte der Nahbereichsphotogrammetrie, Wien, Jänner 2002.

Heft 62 CHMELINA, Wissensbasierte Analyse von Verschiebungsdaten im Tunnelbau. Dissertation, 2002.

Heft 63 NIESSNER, Qualitative Deformationsanalyse unter Ausnutzung der Farbinfor-Mation. Dissertation, 2002.

Heft 64 K.BRETTERBAUER, R.WEBER, A Primer of Geodesy for GIS-Users. October 2003.

Heft 65 N.PFEIFER, 3D Terain Models on the basis of a triangulation, Wien, Jänner 2002.